Flow of mass and energy in the magnetospheres of Jupiter and Saturn

Fran Bagenal[1,2] and Peter A. Delamere[1]

Received 16 November 2010; revised 23 January 2011; accepted 18 February 2011; published 17 May 2011.

[1] We present simple models of the plasma disks surrounding Jupiter and Saturn based on published measurements of plasma properties. We calculate radial profiles of the distribution of plasma mass, pressure, thermal energy density, kinetic energy density, and energy density of the suprathermal ion populations. We estimate the mass outflow rate as well as the net sources and sinks of plasma. We also calculate the total energy budget of the system, estimating the total amount of energy that must be added to the systems at Jupiter and Saturn, though the causal processes are not understood. We find that the more extensive, massive disk of sulfur- and oxygen-dominated plasma requires a total input of 3–16 TW to account for the observed energy density at Jupiter. At Saturn, neutral atoms dominate over the plasma population in the inner magnetosphere, and local source/loss process dominate over radial transport out to 8 R_S, but beyond 8–10 R_S about 75–630 GW needs to be added to the system to heat the plasma.

Citation: Bagenal, F., and P. A. Delamere (2011), Flow of mass and energy in the magnetospheres of Jupiter and Saturn, *J. Geophys. Res.*, *116*, A05209, doi:10.1029/2010JA016294.

1. Introduction

[2] Jupiter is the archetype of a rotation-driven magnetosphere dominated by an internal source of plasma. Saturn is similarly dominated by rotation and internal plasma sources but because of a weaker magnetic field the scale of the Saturnian magnetosphere is considerably smaller. These magnetospheres have been traversed by multiple spacecraft where they measured a variety of magnetospheric properties in situ and remotely. The two pairs of Pioneer and Voyager spacecraft flew past Jupiter, three of the four also flying past Saturn; Ulysses, Cassini and New Horizons flew past Jupiter on their way elsewhere; Galileo made 33 orbits of Jupiter and Cassini continues to orbit Saturn. *Bagenal et al*. [2004] and *Dougherty et al*. [2009] review the properties and current theoretical ideas of these magnetospheres.

[3] At Jupiter and Saturn the plasma is produced by the ionization of neutral gases that spew from the volcanic moons Io and Enceladus, respectively. Coupled to the rotating planets by strong magnetic fields, the magnetospheric plasma rotates with the planets' ~10 h spin period. Radial transport by a diffusive flux tube interchange process carries this plasma outward, away from the planet on time scales of weeks. The strong rotational flows produce strong centrifugal forces on the plasma that is subsequently confined to a relatively thin disk.

[4] Of particular importance is the fact that the plasma in the plasma sheets at both Jupiter and Saturn has temperatures on the order of a few keV. A major issue at both magnetospheres has been why does the plasma not cool down as it moves outward and expands into the larger volume of the outer magnetosphere? The need to heat the plasma in the plasma sheet has been known since Pioneer [e.g., *Goertz*, 1976; *Barbosa et al.*, 1979; *Schardt and Goertz*, 1983]. Some ideas have been proposed [*Sentman et al.*, 1975; *Carbary et al.*, 1976; *Nishida*, 1976; *Goertz*, 1978; *Borovsky et al.*, 1981; *Fujimoto and Nishida*, 1990; *Selesnick et al.*, 2001; *Saur*, 2004] but not fully developed.

[5] A current trend of magnetospheric physics is to develop global numerical models, to explore how these giant planet magnetospheres respond to changes in the solar wind [*Gombosi and Hansen*, 2005; *Hansen et al.*, 2005; *Fukazawa et al.*, 2005, 2006, 2010; *Winglee et al.*, 2009; *Zieger et al.*, 2010]. But to date none of these models include the necessary heating to obtain realistic thermal pressures in the plasma, pressures that dominate over the local magnetic field pressure (by up to a factor of 100 for the outer half of Jupiter's magnetosphere). Without realistic values of the plasma pressure no model can capture the basic plasma dynamics. Rather than attempt the tough job of deriving a physical mechanism for heating the plasma, in this paper we try to quantify the amount of heating necessary to produce the observed properties. This will provide the information for modelers to add the necessary heating, albeit perhaps ad hoc, that will allow them to better address issues of the dynamics of these magnetospheres.

[6] Previous attempts to catalog the mass and energy budgets through the magnetosphere of Jupiter were made by *Krimigis et al*. [1981] and *Hill et al*. [1983]. We provide an update on these studies, including data at Jupiter from the Galileo orbiter and Cassini flyby as well as compare with recent observations from Cassini in orbit around Saturn.

[1]Laboratory for Atmospheric and Space Physics, University of Colorado at Boulder, Boulder, Colorado, USA.
[2]Also at Department of Astrophysical and Planetary Sciences, University of Colorado at Boulder, Boulder, Colorado, USA.

0148-0227/11/2010JA016294

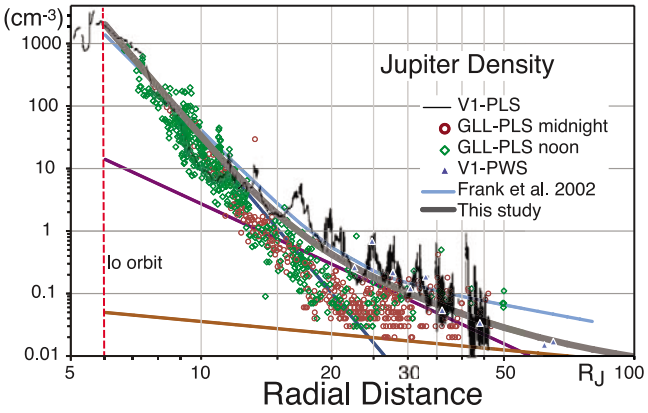

Figure 1. Density measurements derived from Voyager 1 PLS (black line), Voyager 1 PWS (blue triangles), and Galileo PLS (all orbits) obtained ±30° around noon (green diamonds) and ±30° around midnight (red circles). The profile from *Frank et al.* [2002] (pale blue curve, equation (2)) is based on Galileo PLS data from the G8 orbit data obtained on the nightside. The model profile used in this study (thick gray curve, equation (1)) is a composite of three power law profiles (blue, purple, and yellow lines).

[7] In section 2 we present a simple model of an axisymmetric plasma sheet based on in situ observations of the plasma density and temperature and derive basic descriptions of how the latitudinal distribution and total plasma pressure vary with distance from the planet. In section 3 we use this axisymmetric model to quantify the distribution of mass, total mass of the plasma sheet, and discuss current models of the plasma sources. In section 4 we quantify the distribution of energy in the plasma sheet and estimate the sources and losses. Finally, in section 5 we summarize our findings.

2. Simple Model of Plasma Sheet

[8] We first derive simple descriptions of the approximate conditions (density, temperature, latitude distribution, and thermal pressure) in the Jovian and Saturnian plasma disks. We know that there are significant variations with local time and longitude (see review chapters of *Dessler* [1983], *Bagenal et al*. [2004], and *Dougherty et al*. [2009]). For the initial purposes of deriving the net flow of mass and energy through the system we take a simple, azimuthally symmetric description. Given the orders of magnitude variations in plasma properties with radial distance, we regard the factors of few variations with longitude and local time to be secondary. In the future, important clues about the dynamics of the system will come from examination of deviations from this symmetric model.

2.1. Plasma Density

[9] In Figure 1 we have combined various measurements of density in Jupiter's plasma sheet from the Voyager (1979) and Galileo (1996–2003) missions. The Voyager 1 Plasma Science (PLS) instrument measurements were obtained on the approach to Jupiter in the late morning sector [*McNutt et al.*, 1981; *Bagenal and Sullivan*, 1981]. The Voyager PLS charge densities shown here are derived from a summation of currents measured across the 10–6000 eV energy range. The derived charge density does not depend on assumptions of composition and agrees well with the sum of densities for separate ion species derived by fitting resolved spectral peaks (see appendices A and B of *McNutt et al*. [1981] as well as simultaneous electron measurements [*Scudder et al.*, 1981]. The semiregular factor of ~5 variation in density is due to the flapping of the plasma sheet over the spacecraft. Electron density has also been derived from measurements by the Voyager Plasma Wave (PWS) instrument, recently cataloged by *Barnhart et al*. [2009] These PWS local measurements of charge density have been averaged over radial distances to give 9 points in the outer magnetodisk (>20 R_J) and agree well with the PLS measurements of total charge density.

[10] The Galileo spacecraft orbited Jupiter for 7 years and made extensive measurements of plasma properties in the plasma sheet. We have taken estimates of plasma density derived via statistical moments of measurements from the Galileo Plasma Science (PLS) instrument and archived in the Planetary Data System (W. Paterson, private communication, 2009). We plotted all Galileo data within ±30° of noon and ±30° of midnight. The densities derived from Galileo data beyond about 20 R_J are generally lower than Voyager 1 values. This may be because of the assumption that the mass/charge is 16 in the Galileo analysis. If there are significant numbers of protons in the outer magnetosphere, fitting the Galileo data with both protons and heavy ions may yield higher densities. We point out that the dependence of total charge density on composition is not a strong effect (depending as (charge/mass)$^{1/2}$), and we estimate the net uncertainty to be less than a factor or 2.

[11] We derive a profile (gray line in Figure 1) of equatorial plasma density (n_0, in cm^{-3}) versus radial distance (R, in R_J) that is an approximate average (by eye) of the functional form

$$n_0 = a_1(R/6)^{-b1} + a_2(R/6)^{-b2} + a_3(R/6)^{-b3} \quad (1)$$

where the coefficients are given in Table 1. Figure 1 also shows a power law fit to Galileo PLS data (light blue line)

Table 1. Model Parameters for Jupiter's Plasma Sheet Model Used in This Study

Property	Coefficient	Value
Density (cm^{-3})		
This study (equation (1))	a_1	1987
	b_1	−8.2
	a_2	14
	b_2	−3.2
	a_3	0.05
	b_3	−0.65
Frank et al. [2002] (equation (2))	a_1	3.2×10^8
	b_1	−6.9
	a_2	9.9
	b_2	−1.28
Scale height (equation (6))	a_1	−0.116
	a_2	2.14
	a_3	−2.05
	a_4	0.491
	a_5	0.126
Azimuthal flow (km/s)	V_{co}	12.6 km/s per R_J
<28 R_J	a_1	1.12
	a_2	1/50
>28 R_J		200 km/s

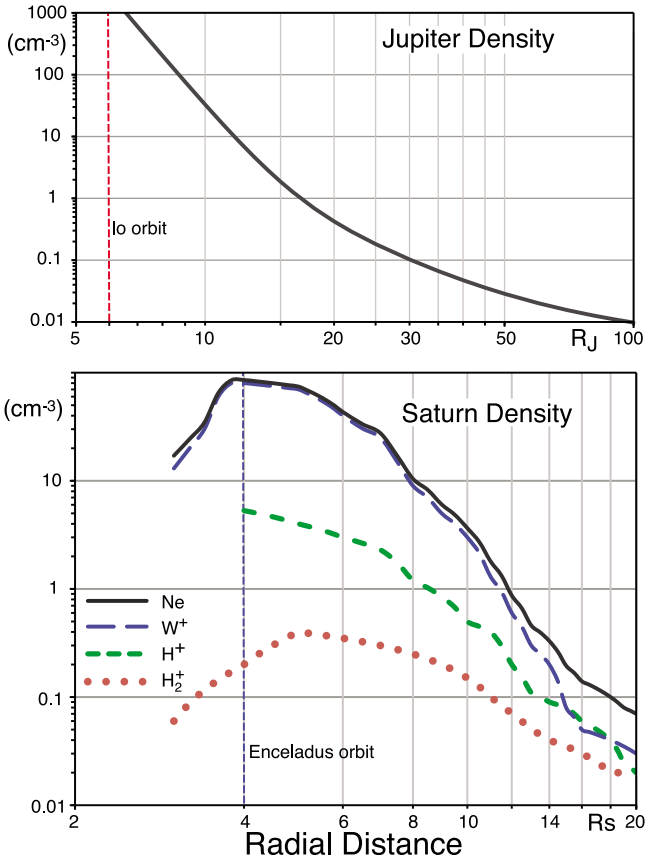

Figure 2. Density profiles for (top) Jupiter and (bottom) Saturn. The model profile for Jupiter was derived from data shown in Figure 1. The densities at Saturn are derived from Cassini CAPS data (<5 R_S) by *Sittler et al.* [2008] and (>5 R_S) by *Thomsen et al.* [2010].

obtained on the G8 orbit in the magnetotail presented by *Frank et al.* [2002] with the functional form

$$n_{\text{Frank02}} = a_1 R^{-b1} + a_2 R^{-b2} \quad (2)$$

where the coefficients are given in Table 1. Our model profile somewhat underestimates the peak densities in the outer plasma sheet, but we show in section 3.1 that this does not significantly affect our estimates of mass and energy flows in the system.

[12] In Figure 2 we compare the plasma sheet density profile for Jupiter described in Figure 1 with a profile of plasma density derived from Cassini CAPS ion data at Saturn. The profiles represent the peak density, n_0, in the center of the plasma sheet. The Saturn values outside ~5 R_S are from *Thomsen et al.* [2010], who took statistical moments for data obtained October 2004 through March 2009. The profiles in Figure 2 (bottom) are derived from measurements taken at low latitudes and when the corotational flow was in the CAPS field of view [*Thomsen et al.*, 2010, Figure 3c]. To push the profiles inward of 5 R_S we took density values from an earlier analysis of CAPS data by *Sittler et al.* [2008]. Similar plasma densities were found by the Voyager PLS instruments when they flew through the system in 1980 and 1981 [*Richardson*, 1986; *Richardson and Sittler*, 1990] as well as derived from Cassini CAPS ELS by *Schippers et al.* [2008], from Cassini RPWS measurements by *Persoon et al.* [2009] and from the Cassini Langmuir probe by *Morooka et al.* [2009]. Allowing for uncertainties in the measurement plus spatial and temporal variability, we consider these values to have a confidence of about a factor of 2.

2.2. Temperature

[13] In Figure 3 we plot ion temperatures derived by the PLS instruments on Voyager 1 (black) and Galileo (green). We ignore electrons because they tend to be much colder than the ions at both Jupiter [*Scudder et al.*, 1981] and Saturn [*Sittler et al.*, 1983], and we are primarily concerned with total thermal energy density in this paper. Ion temperatures tend to be less well determined than other plasma properties such as flow and density. This is partly because of the assumptions that must be made about ion composition but the derived temperatures also tend to depend on the energy range of the measuring instrument (10 eV to 6 keV for Voyager, 1 eV to 52 keV for Galileo). For example, if one looks at the plots of temperature derived from the Voyager PLS data [e.g., *Belcher*, 1983, Figure 3.13] one sees low temperatures (~10 eV) in places (usually where the density is higher) out to as far as 40 R_J. Away from these relatively small regions of cold dense plasma the Voyager PLS instrument recorded a fairly constant temperature of the heavy ions of ~100 eV. Note that S^+ and S^{++} or O^+ ions moving at 200 km/s have kinetic energy of 6.6 keV and 3.3 keV so that if they have temperatures >100 eV, much of the flux is above the 6 keV limit of the Voyager PLS instrument. On the other hand, when one looks at the Galileo PLS observations one sees a wider range in temperatures, particularly in the outer plasma sheet. We only show the temperatures around noon in Figure 3. The data around midnight showed even greater scatter. Further work is needed to ascertain whether this is a true variation between the Voyager

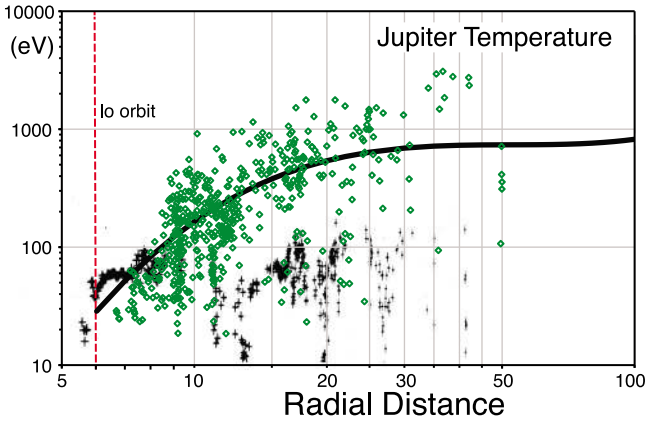

Figure 3. Temperature of the thermal ions derived at Jupiter from the Galileo PLS data obtained ±30° around noon (green diamonds) and from Voyager 1 PLS data (black crosses, *McNutt et al.* [1981]). The model profile used in this study (black curve) is derived beyond ~10 R_J from estimates of the vertical scale height of density in the plasma sheet (see equations (3) and (4)).

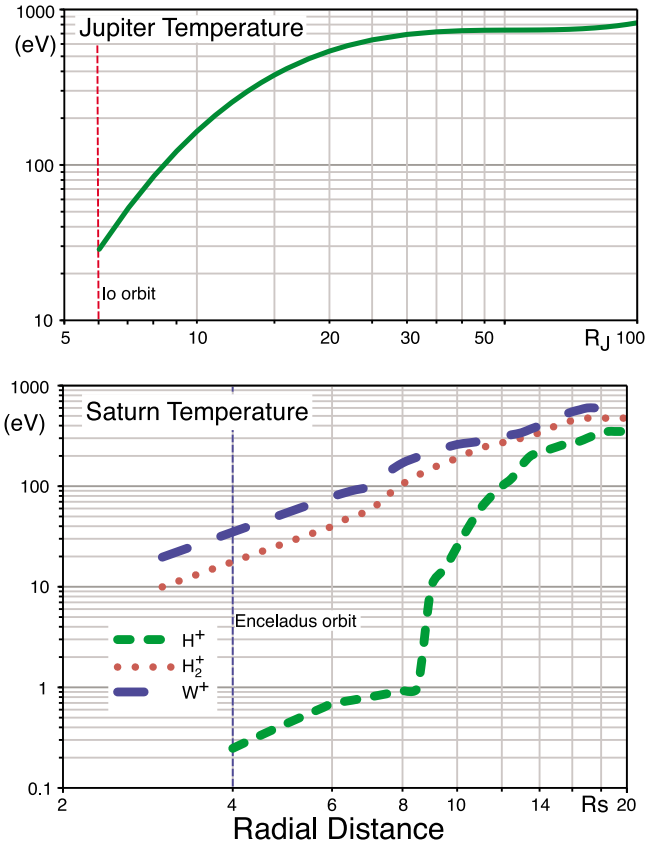

Figure 4. Temperature of the thermal ions at (top) Jupiter (see Figure 3) and (bottom) Saturn. The Saturn profile is derived from the Cassini CAPS data [*Thomsen et al.*, 2010; *Sittler et al.*, 2008].

and Galileo epochs or primarily a consequence of the higher upper energy range of Galileo over Voyager. It is also possible that there are small blobs of cold (10–100 eV) plasma embedded in a warmer background.

[14] A major part of the issue in defining what one means by ion temperature is that the velocity distributions of the plasma ions are not pure Maxwellian distributions. There is substantial evidence of a significant tail to the distribution at suprathermal energies [e.g., see *Krimigis and Roelof*, 1983, Figure 4.14]. When we come to consider the plasma pressure and thermal energy density we will need to include this suprathermal component.

[15] For simplicity, we use the power law derived for scale height (H, in R_J, see equation (6)) and assume that a characteristic temperature T (in eV) is

$$T = \mathrm{Ai}(H/0.64)^2 \tag{3}$$

where we assume the average ion mass, Ai, is 20 amu corresponding to a mixture of sulfur and oxygen ions. Uncertainties in the composition plus the measured scale height suggest uncertainties in the derived temperatures of about a factor of at least 2. Figure 3 shows an example of the scatter in the temperature data at Jupiter.

[16] Figure 4 shows radial profiles of temperature at Jupiter and Saturn. The model profile shown for Jupiter is derived as described in section 1. The Saturn profile comes from *Thomsen et al.* [2010, Figure 8] as well as from *Sittler et al.* [2008] for values inside ~5 R_S. Both sources quote temperature of the water group ions (W+) increasing as R to approximately the second power. In both Jovian and Saturnian cases the ion temperature increases with radial distance. This is completely contrary to the expectation that the plasma would cool as it plasma expands into a larger volume, clearly showing that the expansion is not adiabatic and that energy must be added to the system, as we discuss further in section 2.4.

2.3. Scale Height

[17] In a rotation-dominated magnetosphere the plasma is confined to the farthest location along the magnetic field from the rotation axis. For a plasma where $T_i \gg T_e$ (which holds outside 5.6 R_J at Jupiter, and pretty much everywhere at Saturn), the average ion mass is Ai (in amu), and the magnetic field is dipolar, the functional form for the density distribution with height, H, away from the centrifugal equator is given by [*Hill and Michel*, 1976]

$$n(z) = n_0 \exp -(z/H)^2 \tag{4}$$

$$H = \left[2/3\ kT_i/\left(m_p \mathrm{Ai}\ \Omega^2\right)\right]^{1/2} = H_0[T_i(\mathrm{eV})/\mathrm{Ai(amu)}]^{1/2} \tag{5}$$

where H_0 = 0.64 R_J and 0.59 R_S for Jupiter and Saturn, respectively. More sophisticated descriptions of the distribution are necessary when one is interested in how different ion species are distributed and if one includes temperature anisotropy [e.g., *Bagenal and Sullivan*, 1981; *Bagenal*, 1994; *Persoon et al.*, 2009]. But for our simple plasma sheet model we will limit ourselves to a simple scale height for density.

[18] Strictly speaking, one should also take into account how the fact that the magnetic field is highly stretched from a dipole by Jupiter's strong ring current affects the vertical distribution of plasma, as modeled by *Caudal* [1986] and by *Achilleos et al.* [2010]. On the other hand, if one looks at the variations in density observed when the plasma sheet flaps past the spacecraft (Figure 1) then one can derive an effective scale height from measuring the height excursion for an e-folding drop in density. By looking at several plasma sheet crossings made by Voyager and by Galileo, we derive a simple scale height function for the Jovian plasma sheet

$$h = a_1 + a_2\ r + a_3\ r^2 + a_4\ r^3 + a_5\ r^4 \tag{6}$$

where h = log10(H) and r = log10(R) and the coefficients are given in Table 1.

[19] Figure 5 shows a comparison of effective profiles of scale height for Jupiter and for Saturn. The Jovian profile is derived as discussed in section 2.1 The Saturnian profile comes from *Thomsen et al.* [2010, Figure 7a] for distances > 6 R_S and from *Persoon et al.* [2009, Figure 13] inside 6 R_S. *Morooka et al.* [2009] similarly derived from Cassini Langmuir probe data empirical functions for the vertical distribution of density that are similar to those of *Thomsen et al.* [2010] and *Persoon et al.* [2009] on the dayside but suggested that the sheet is thinner on the nightside, perhaps due to dayside solar wind compression.

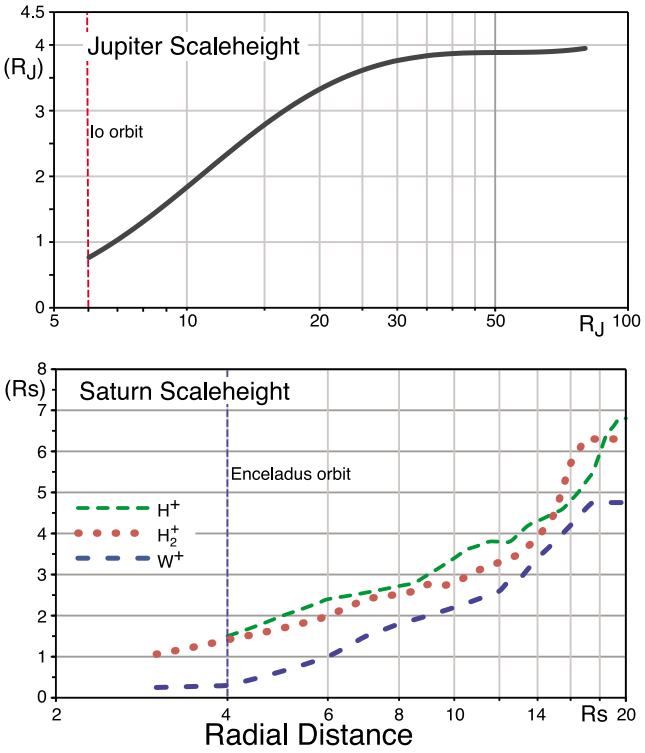

Figure 5. Scale heights of plasma density at (top) Jupiter (equation (6)) and (bottom) Saturn.

2.4. Pressure

[20] For the thermal plasma that dominates the density in the plasma sheet, with temperatures of 10 eV to 1 keV, we calculate the local thermal pressure as P = nkT. Radial profiles of local plasma pressure are calculated from equatorial density, n_0 (Figure 2), and temperature (Figure 4) and shown in Figure 6 for Jupiter and Saturn. Pressure can also be derived from measurements of fluxes of particles at higher energies. At Jupiter it is these 20 keV to 50 MeV particles, particularly sulfur ions, that dominate (by about a factor of 10) the pressure in the Jovian plasma sheet [e.g., *Mauk et al.*, 2004]. The measured intensities of these more energetic particles rapidly drops inside about 10 R_J. Modeling the fluxes of energetic neutral atoms coming from the Jovian system [*Mauk et al.*, 2003] suggests that the energetic ions are lost due to charge exchange with the extended neutral cloud that extends from Io out beyond the orbit of Europa.

[21] At Saturn, *Sergis et al.* [2009, 2010] calculate the pressure of energetic (>3 keV) ions from Cassini MIMI data. The average radial pressure profile of *Sergis et al.* [2010, Figure 11] is shown in Figure 6. The energetic particle pressure is greatly reduced at Saturn but they contribute more pressure than the thermal plasma beyond ~11 R_S. We suggest this difference of Saturn from Jupiter is partly due to higher density of neutrals removing energetic particles via charge exchange as they move inward, as well as perhaps a weaker heating process in Saturn's smaller magnetosphere.

[22] At Jupiter the high plasma pressures in the plasma sheet dominate the local magnetic field pressure producing values of $\beta = P/(B^2/2\mu_0)$ greater than unity beyond ~15 R_J, increasing to greater than 100 at 45 R_J [*Mauk et al.*, 2004]. Early attempts to calculate the radial forces on the plasma found that centrifugal forces of the rotating thermal plasma could not balance the magnetic stresses [*McNutt*, 1984; *Mauk and Krimigis*, 1987] which *Paranicas et al.* [1991] later found could be balanced with pressure gradient forces associated with the 20–200 keV plasma population. Not only does the plasma pressure dominate the magnetic pressure, but the radial profile of plasma pressure is also considerably flatter than the $1/R^6$ variation in magnetic pressure for a dipole field. It is the high plasma pressure in the plasma disk that doubles the scale of Jupiter's magnetosphere from the dipolar stand-off distance of ~42 R_J to 65–90 R_J. The shallow gradient in plasma pressure accounts for the high compressibility of the magnetosphere with the subsolar magnetopause varying as solar wind ram pressure to the −1/~4.5 power, rather than −1/6 power for a magnetic dipole [*Slavin et al.*, 1985; *Huddleston et al.*, 1998; *Joy et al.*, 2002; *Alexeev and Belenkaya*, 2005]. *Delamere and Bagenal* [2010] argue that the high-beta plasma inside Jupiter's magnetosphere limits the solar wind interaction to a viscous boundary layer.

[23] At Saturn the plasma pressures are less than Jupiter but the plasma beta is still greater than unity beyond 8 R_S [e.g., *Sergis et al.*, 2010] and has values of 2–5 in the plasma sheet. *Chou and Cheng* [2010] recently built a model

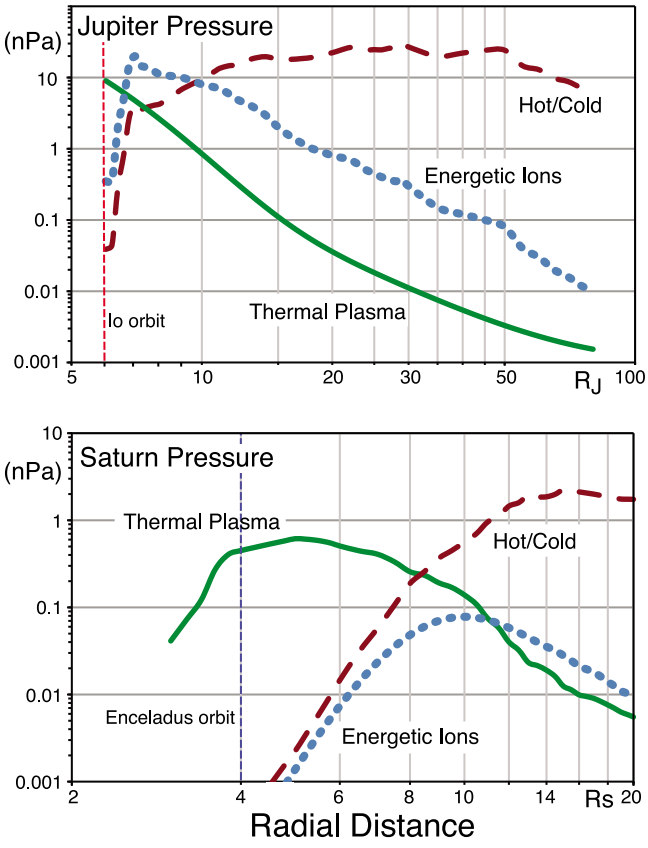

Figure 6. Profiles of thermal pressure of the thermal (green solid) and energetic (blue dotted) ion populations at (top) Jupiter and (bottom) Saturn. The ratio of hot/cold (red dashed) is the ratio of the energetic population pressure to that of the thermal pressure.

Table 2. Flow of Mass Through the Jovian and Saturnian Magnetospheres

	Jupiter	Saturn	J/S
Mass of neutrals	~70 kt	~1 Mt	~1/14
Mass of plasma	1.5 Mt	83 kt	18
Plasma production	260–1400 kg/s	12–250 kg/s	1–120
Neutral production	600–2600 kg/s	70–750 kg/s	1–40
Fast neutral loss	320–1740 kg/s	20–300 kg/s	1–90
Plasmoid loss	~30 kg/s	??	??
Solar wind flux[a]	150 t/s	3 t/s	46

[a]Flux of solar wind onto area of πR_T^2 where R_T = magnetopause distance at terminator (~120 R_J, ~38 R_S).

of the Saturnian plasma sheet based on Voyager PLS data and derived rather lower values ($\beta < 1.2$ for Voyager 1, < 2.5 for Voyager 2) but they are missing the contributions of energetic ions. The significant contributions of suprathermal ions to the plasma pressure have, however, been incorporated in most models of the structure and dynamics of Saturn's plasma sheet [*Arridge et al.*, 2007, 2008; *Achilleos et al.*, 2010; *Sergis et al.*, 2010; *Kellett et al.*, 2010] The more modest values of beta at Saturn are consistent with the magnetopause stand-off distance varying as −1/5 power of solar wind pressure, as found by *Kanani et al.* [2010].

3. Mass: Distribution, Sources, and Flux

[24] Armed with a simple model of plasma density in the plasma disk we can estimate the flow of mass through the system, compared in Table 2 for Jupiter and Saturn.

3.1. Total Mass

[25] We can now take our radial profiles of plasma density in the center of the sheet, n_0, plus the scale height, H, and integrate vertically and azimuthally to obtain the radial distribution of mass (per meter of radial distance)

$$M(R) = 2\ \pi^{3/2}\ n_0\ \mathrm{Ai}\ m_p\ H\ R \qquad (7)$$

where Ai is the average ion mass and m_p is the mass of the proton. Integrating the profile outward we can estimate the cumulative mass of the plasma disk. At Jupiter, the 1.5 Mt of net mass of plasma is found predominately in a narrow region (6–6.5 R_J) in the Io plasma torus while the 83 kt of plasma mass in the Saturn system is spread out from 4 to 9 R_S (see Figure 7). We estimate our confidence in these numbers to be about a factor of a few. Hence, our Saturn estimate is consistent with the 50 kt value of *Chen et al.* [2010].

[26] Since we know the majority of the magnetospheric plasma came from the ionization of neutral clouds coming from Io and Enceladus, it is useful to estimate the total mass of the neutral clouds. At Jupiter the neutral clouds of sulfur and oxygen are hard to detect and rarely observed (see review by *Thomas et al.* [2004]). The distribution of molecular SO_2, SO or S_2 are even harder to detect. Models of the neutral cloud by *Smyth and Marconi* [2005] estimate the total mass of neutral oxygen and sulfur atoms from Io to comprise ~52 kt with another ~17 kt of water products from Europa to total ~70 kt of neutrals in the Jovian system. The denser neutral cloud at Saturn is more easily observed via UV emissions: of O and H by Cassini UVIS [*Melin et al.*, 2009; *Shemansky et al.*, 2009] and of OH by Hubble Space Telescope (HST) [*Shemansky et al.*, 1993]. Estimates from observations and models suggest a total mass of ~1 Mt of material (water molecules and dissociation products) in the neutral clouds [*Shemansky et al.*, 2009; *Cassidy and Johnson*, 2010].

[27] The masses of neutrals and of plasma in Table 2 dramatically show the contrast in these two systems. Jupiter has a massive plasma disk with little remaining neutral, while at the Saturn system most of the material remains in a massive, spread out neutral cloud with only a modest fraction being ionized. At Jupiter, ions outweigh neutrals by 20:1, while at Saturn, neutrals outweigh ions by 12:1. *Delamere et al.* [2007] argue that this major (factor of ~250) difference in the ion:neutral ratio between the two systems arises primarily because of the factor of 2 lower speed of plasma flowing past Enceladus compared with Io. The subsequent factor of 4 lower pickup energy means that there is insufficient energy to adequately ionize the neutral cloud at Saturn. Moreover, molecular dissociative recombination (e.g., $H_2O^+ + e^- \rightarrow OH + H$) introduces a sink of plasma at Saturn that does not exist (except perhaps very close to Io) at Jupiter.

3.2. Satellite Sources and Losses

[28] Contrary to common misconceptions, only a small fraction of the plasma at both Jupiter and Saturn come

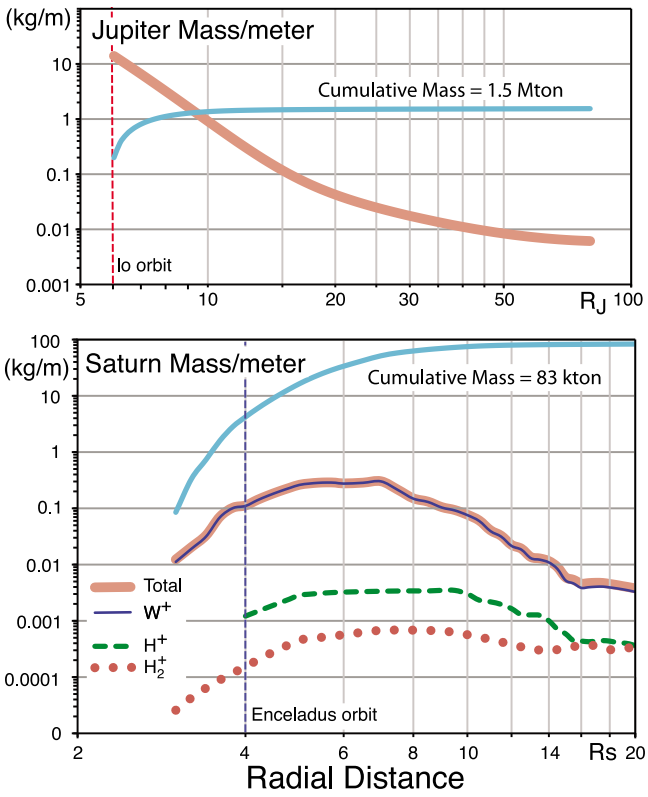

Figure 7. Distribution of mass in the plasma sheets of (top) Jupiter and (bottom) Saturn. The plasma mass has been integrated over a uniform annulus of radius R, scale height H, and width of a meter. This mass/meter profile (pink curve) is then integrated radially outward to provide a total cumulative mass (pale blue curve).

Table 3. Variability of the Io Plasma Torus Based Physical Chemistry Models of UV Emissions[a]

	Voyager 1 Mar 1979	Voyager 2 Jul 1979	Cassini Sep 2000	Cassini Jan 2001
Neutral source Mdot (t/s)	0.8	2.6	3.0	0.6
Time scale τ (days)	50	23	14	64
Oxygen/sulfur	4	4	1.9	1.9
Hot electrons (%)	0.23	0.12	0.25	0.25
Power emitted (TW)	1.2	2.5	2.0	1.5

[a]From *Delamere and Bagenal* [2003], *Steffl et al.* [2006], and *Delamere et al.* [2004].

directly from the atmospheres of their volcanic moons but, rather, arises from ionization of clouds of neutrals that extend a substantial fraction of the way around the planet (see reviews by *Thomas et al*. [2004] for Jupiter and *Shemansky et al*. [1993], *Jurac and Richardson* [2005], and *Cassidy and Johnson* [2010] for Saturn). For each planet we discuss current models of the neutral clouds and plasma tori.

[29] The best constraints on the plasma production in the Io plasma torus comes modeling the physical chemistry of a mixture of neutrals, ions and electrons and tying them to UV emissions observed remotely [*Shemansky*, 1988; *Barbosa*, 1994; *Schreier et al.*, 1998; *Lichtenberg and Thomas*, 2001). More recently, *Delamere and Bagenal* [2003] used a homogeneous model of the torus physical chemistry to model the data from the Voyager 1 and Voyager 2 flybys in 4 months apart 1979, as well as the time of Cassini closest approach to Jupiter in January 2001. *Krüger et al.* [2003] subsequently reported a 3 order of magnitude increase in dust production from the Jovian system, peaking in August-September 2000, before Cassini arrived at Jupiter. This raised the question of whether the plasma torus experienced a similar thousandfold increase in source. *Delamere et al.* [2004] modeled the decrease in UV emissions from the torus observed through the end of 2000 by the Cassini UVIS [*Steffl et al.*, 2004] to derive plasma conditions at the peak plasma production (September 2010) and found that the required increase in iogenic neutral gas was only around a factor of 3. It is intriguing whether such a high ratio for production of dust compared to plasma production is typical or is expected to vary with type (and/or epoch) of volcanic eruption.

[30] Table 3 shows the Io torus model parameters for the two Voyager and two Cassini epochs, and Figure 8 shows the corresponding flow of mass and energy through the torus. The conditions during Voyager 1 (March 1979) and at Cassini closest approach (January 2001) are fairly similar and may represent typical conditions. During the Voyager 2 (July 1979) and Cassini September 2000 periods the torus seems to have had a higher source strength as well as more rapid radial transport (net time scale of 14–23 days rather than the 50–64 days of Voyager 1 and Cassini January 2001). The net production of neutral material needed from Io to match these four cases ranges from 0.7 to 3 t/s. The quantity of plasma transported out of the torus is 0.26 t/s (Voyager 1) to 1.4 t/s (Cassini outburst), a range of a factor of 5. Note in Figure 8 that only 1/3 to 1/2 of the initial neutral source remains ionized and transported out to the plasma sheet. The other 2/3 (to 1/2) of the mass is lost via charge exchange within the corotating torus ions and escapes the system as fast neutrals. The shift in the oxygen/sulfur ratio from ~4 for the Voyager epoch to a factor of 1.9 at the

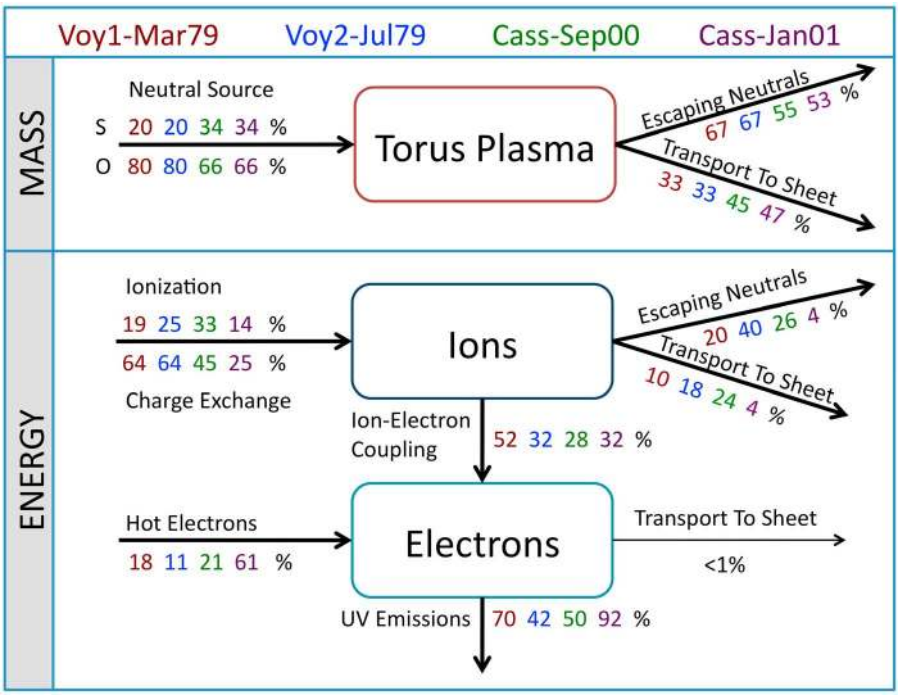

Figure 8. Schematic diagram of the mass and energy flow through the Io plasma torus from models constructed to match observations made at the time of the Voyager and Cassini flybys. Based on the works by *Delamere and Bag*enal [2003], *Delamere et al.* [2004], and *Steffl et al.* [2006].

Table 4. Enceladus Neutral Sinks

	Jurac and Richardson [2005]	*Cassidy and Johnson* [2010][a]	*Fleshman et al.* [2010c][b]
Neutral source (kg/s)	300	300	150
Lost to Saturn and rings (%)	27	43	44
Plasma production (%)	38	26	17
Fast neutral loss (%)	24	31	39

[a]Model includes neutral-neutral collisions plus charge exchange with cross section depending on average speed of populations.
[b]Charge exchange scattering of individual particles with cross section depending on relative speed of individual ions and neutrals.

time of Cassini may be related to the composition of the volcanic gases at these times. But until we understand the details of how gases from the atmosphere of Io interact with the streaming plasma and are dispersed as extended neutral clouds such causal explanations are highly speculative.

[31] At Saturn, estimates of the total neutral production rate of water molecules (presumably ultimately coming from Enceladus' plumes) vary around the initial value of 300 kg/s, determined from the initial UV occultation of the plume by *Hansen et al*. [2006]), which is the same as from the earlier *Jurac and Richardson* [2005] model constructed to match HST observations of the OH neutral cloud. *Sittler et al.* [2008] preferred 600 kg/s but only claimed a factor of 2 accuracy, so this value is still consistent with *Hansen et al*.'s [2006] 300 kg/s. *Saur et al*. [2008] modeled the electrodynamics of the plume deriving values as high as 1600 kg/s for E0 and as low as 200 kg/s for E1 and E2. Meanwhile, a value of ~200 kg/s was derived from a second UV occultation reported by *Hansen et al*. [2008]. Similarly, *Fleshman et al*. [2010b] found 100–180 kg/s was consistent with their physical chemical modeling of the Enceladus torus. Finally, *Smith et al*. [2010] have analyzed INMS data from three Cassini flybys of Enceladus from which they conclude that the net production has increased by a factor of 10 from <72 kg/s (at the time of E2, July 2005) to 190 kg/s (at E3) to 750 kg/s (at E5, October 2008). This is contrary to presentations by *Hansen et al*. [2010], who claim only ~25% variations in the plume over three stellar occultations by Cassini UVIS in February 2005 (170 kg/s), July 2005 (220 kg/s), and October 2007 (180 kg/s).

[32] The fate of the neutrals is more complicated at Saturn than Jupiter. The high neutral-to-ion density ratio at Saturn is a result of lower ionization rates (caused as much by photoionization ionization at Saturn as electron impact ionization that dominates at Jupiter). Only a fraction of the neutral material is transported out into the plasma sheet. Some of the corotating ions charge exchange with neutrals to become escaping fast neutrals but other collisional processes such as photodissociation and electron-dissociation, neutral-neutral collisions and low-velocity charge exchange "puff" up the neutral cloud, spreading it beyond Enceladus' orbit (4 R_S) as well as sending a substantial flux of neutrals into the planet Saturn. To summarize the current models of neutral loss processes at Saturn, we have taken the Voyager/HST-based neutral cloud model of *Jurac and Richardson* [2005], and we compare their results in Table 4 with Cassini era neutral cloud models of *Cassidy and Johnson* [2010] and of *Fleshman et al*. [2010c]. Table 4 lists estimates from the three different models of the fraction of the neutrals that are lost to ionization, that are ejected from the Saturn system or sent into the planet or rings. The differences in these models are due to different ways that the various collisional processes are handled in the neutral cloud models. These models calculate the physical chemistry of the Enceladus torus for neutral production rates of 150 or 300 kg/s.

[33] At Saturn, it is not clear that the rate of ionization versus other neutral loss processes would be maintained at the modeled fractions if the neutral source increases to *Smith et al.*'s [2010] E5 values of ~750 kg/s or *Saur et al.*'s [2008] E0 value of 1600 kg/s. One might expect that as neutral production increases neutral-neutral collisions would cause more of the material to escape as neutrals rather than be ionized. Electron impact ionization would be reduced due to collisional cooling of the electrons. In fact, *Tokar et al.* [2009] do not report higher than average plasma densities around the time of E5. Nevertheless, if we assume that something between 17% [*Fleshman et al.*, 2010c] and 38% [*Jurac and Richardson*, 2005] of the neutral source becomes ionized, then the 70–750 kg/s range in neutral source produces a net plasma source at Saturn ranging from 12 to as much as 250 kg/s (see Table 2). *Pontius and Hill* [2009] estimated 100 kg/s, and recently, *Chen et al.* [2010] used observed plasma density and radial flow speeds to suggest a value of plasma outflow of 280 kg/s. *Liu et al.* [2010] simulated Saturn's plasma disk with the Rice Convection Model and a derived mass flux of ~35 kg/s. We hope that as models evolve and Cassini continues to take measurements the story of the Enceladus torus and its variability will solidify.

[34] Figure 9 compares the flow of mass and energy (discussed in section 4) through the Jovian and Saturnian systems. The model matching the conditions at the time of Voyager 1, often taken as "typical" of the torus, have been used for the Jupiter case (taken from *Delamere and Bagenal* [2003]). For the Saturn case we use the range of mass flows from the three models summarized in Table 4.

[35] *Vasyliūnas* [2008] uses simple scaling relationships to argue that when the plasma production at these planets is compared with the solar wind source or to a critical mass loading to argue that plasma production at Saturn is relatively more important than at Jupiter. His simple analysis ignores, however, the important effects of (1) plasma heating on dynamical behavior and (2) equatorial confinement of the plasma leading to decoupling of the plasma in the magnetosphere (rather than in the ionosphere).

3.3. Nonsatellite Sources

[36] While the Jovian and Saturnian systems are noted for their internal source of plasma from their volcanic moons, it must be pointed out that the flux of solar wind plasma intersected by these vast magnetospheres is substantial. Table 2 shows that even if only a fraction of a percent leaks into the magnetosphere the net source of solar wind plasma would be comparable to the satellite sources. The

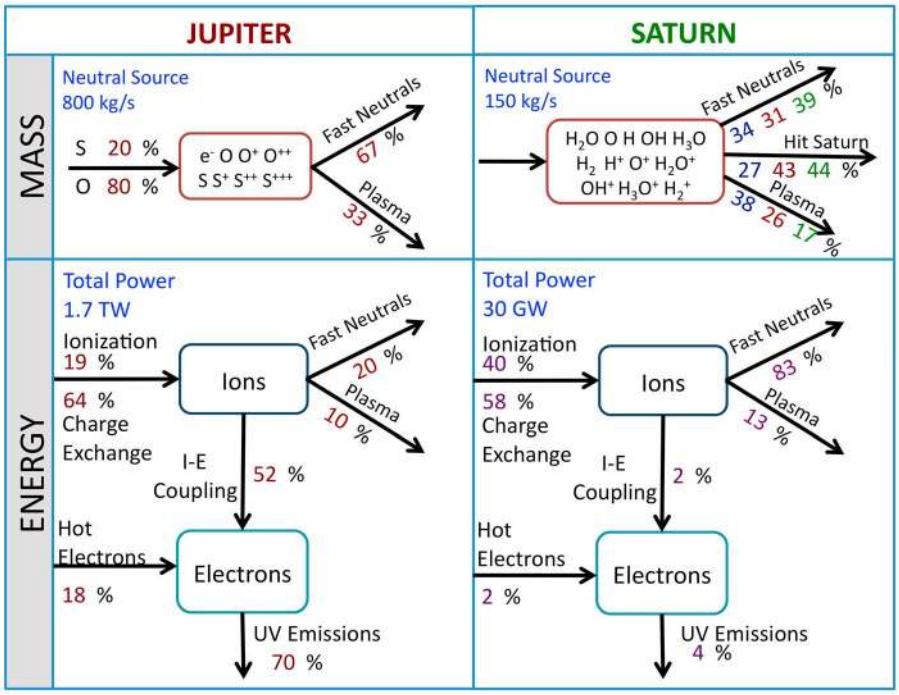

Figure 9. Schematic diagrams comparing the mass and energy flow through the ((left) Jovian and (right) Saturnian systems. The models matching the conditions at the time of Voyager 1 have been used for the Jupiter case (Figure 8). For Saturn, the neutral loss rates in blue, red, and green come from the models of *Jurac and Richardson* [2005], *Cassidy and Johnson* [2010], and *Fleshman et al.* [2010c], respectively. The energy flow for Saturn is from *Fleshman et al.* [2010b].

dominance of heavy ions in the inner/middle magnetospheres indicates that little solar wind plasma penetrates very far inside. But in the outer regions of these magnetospheres light ions are abundant, including He^{++}, and other ions of solar origin such as O^{6+} [*Hamilton et al.*, 1981; *Bame et al.*, 1992; *Cohen et al.*, 2001].

[37] Beyond the source regions (4–6 R_S for Saturn, 5.8–6.5 R_J for Jupiter) the density profiles drop steeply as the plasma spreads out into the region surrounding the planet. The enhanced abundance of light ions at the outer edges of the plasma disk (17–20 R_S) led *Thomsen et al.* [2010] to suggest ionization of hydrogen from Titan's upper atmosphere. We believe that the lifetimes for ionization are too long to make this probable and suggest penetration of solar wind plasma into Saturn's dayside, consistent with recent studies of leakage across the magnetopause due to Kelvin-Helmoltz vortices, particularly on the dawn flank [*Masters et al.*, 2009; P. A. Delamere et al., The Kelvin-Helmholtz instability in Saturn's outer magnetosphere, unpublished manuscript, 2011]. At Jupiter, the plasma density profile starts steep but flattens out considerably beyond 20–30 R_J, just a third of the distance out to the dayside magnetopause (average subsolar distance of 66–92 R_J according to *Joy et al.* [2002]). The shallower gradient in the outer plasma sheet may indicate a source of material from the solar wind [*Delamere and Bagenal*, 2010].

[38] The ion composition of the boundary layers inside of the magnetopause is also consistent with mass transport at the magnetopause. At Jupiter *Bame et al.* [1992] reports on ion composition in the boundary layer during the expansion of the magnetopause past the Ulysses spacecraft. The magnetopause was not a sharp spatial boundary, rather magnetosheath and magnetospheric populations were observed to coexist within the boundary layer internal to the magnetopause. A boundary layer was clearly present for all but one of the Jovian magnetopause crossings. Similarly, *Galvin et al.* [1993] and *Phillips et al.* [1993] reported a mixed boundary layer composition, and *Galvin et al.* [1993] suggested that transport across the magnetopause boundary can work both ways. A significant finding by *Hamilton et al.* [1981] from the Voyager 2 LECP data is that the plasma sheet composition beyond 60–80 R_J in the tail is similar to that of solar wind energetic ions while the inner magnetosphere is dominated by iogenic material. *Krupp et al.* [2004a] discussed evidence of a boundary layer seen in the Cassini MIMI/LEMMS energetic electron data when Cassini skimmed Jupiter's dusk magnetopause during the gravity assist flyby. They suggest that the leakage of energetic magnetospheric electrons to the magnetosheath is consistent with open field lines planetward of the magnetopause. Most recently, the particles measured by New Horizons as it traversed down the flanks of the magnetotail were increasingly dominated by light ions at farther distances down tail [*Haggerty et al.*, 2009; *Hill et al.*, 2009; *Ebert et al.*, 2010].

[39] While we support the view that large-scale, persistent reconnection (as in a Dungey-style solar wind driven convection system) is unlikely at Jupiter [*McComas and Bagenal*, 2007], there is gathering support of small-scale,

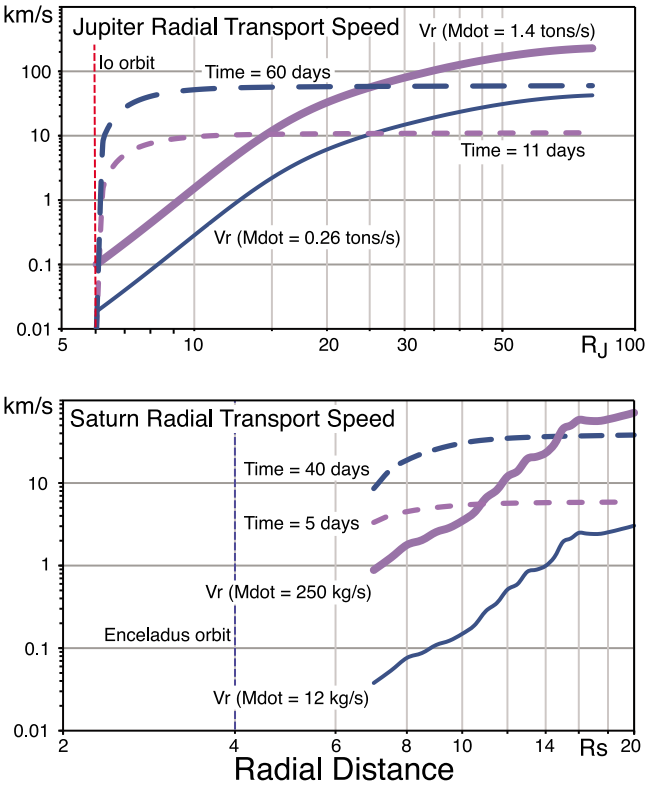

Figure 10. Radial transport rates for (top) Jupiter and (bottom) Saturn derived from conservation of flux and measurements of the radial profile of mass density (Figure 7).

intermittent reconnection (e.g., as in shear-driven Kelvin-Helmholtz instabilities) occurring at both Jupiter [*Delamere and Bagenal*, 2010] and Saturn [*Goertz*, 1983; *Masters et al.*, 2009; Delamere et al., unpublished manuscript, 2011].

[40] *Hill et al.* [1983] estimated the solar wind source by taking the fraction of solar wind leaking into the magnetosphere of $\sim 10^{-3}$ and obtained a tiny source strength of 20 kg/s for a radius of cross section of 100 R_J. We took a more realistic cross section of the terminator of 120 R_J, a local solar wind density of 1 cm^{-3} and speed of 400 km/s and estimated a solar wind flux of ~150 t/s which makes a source of 150 kg/s for the *Hill et al.* [1983] 0.1% leakage rate. For Saturn, allowing for the $1/R^2$ decrease in solar wind density and the smaller cross section (taken as 38 R_S) and using the same 0.1% leakage rate, we found a potential solar wind source of $10^{-3} \times 3$ t/s = 3 kg/s. This is comparable to estimates derived by Delamere et al. (unpublished manuscript, 2011) from a hybrid simulation of diffusive transport across the magnetosphere driven by Kelvin-Helmholtz instability. Even with such low mass source rates, the enhanced density of protons will significantly alter the ion composition of the outer boundary layers.

[41] Finally, it must be noted that the giant planets themselves may be sources of plasma. At Jupiter the most convincing evidence comes from *Hamilton et al.* [1981], who report fluxes in the Jovian magnetosphere of He^+ and H_3^+ ions which most likely come from Jupiter's ionosphere. The outflow of ionospheric plasma was proposed by *Nagy et al.* [1986] and estimated to be 2×10^{28} ions/s which is comparable in number density to the iogenic source but, assuming the composition is mostly protons, the mass would be only 35 kg/s.

[42] At Saturn, the presence of water dissociation products with similar masses as ionospheric ions makes the distinction of the different sources even harder. *Krimigis et al.* [2005] report an abundance of He^+ ions that is far great than He^{++} particles in Saturn's plasma sheet, consistent with an ionospheric source. *Glocer et al.* [2009] modeled potential ionospheric outflow at Saturn and estimated the source to be only a few kg/s. We hope that the polar passes by Cassini at Saturn and the Juno mission to Jupiter will determine the amount of outflowing ionospheric material from these gas giant planets.

3.4. Radial Transport

[43] The plasma in the outer planet magnetospheres is believed to be transported radially outward via centrifugally driven flux tube interchange [e.g., *Hill et al.*, 1981]. At Jupiter, while many have looked, direct evidence of the instability has been very rare [*Thorne et al.*, 1997; *Bolton et al.*, 1997; *Kivelson et al.*, 1997; *Frank and Paterson*, 2000], but at Saturn the weaker field has allowed observation of many flux interchanges [*André et al.*, 2005; *Burch et al.*, 2005; *Hill et al.*, 2005; *Mauk et al.*, 2005; *Chen and Hill*, 2008]. In the Io plasma torus, for each species there are radially distributed sources (e.g., the extended neutral cloud) and losses (e.g., charge exchange) so that one needs to solve a self-consistent system suffering both physical chemistry and diffusive transport. But beyond ~6.5 R_J sources and losses due to the collisional processes become insignificant. Saturn's neutral clouds are more spread out but collision rates drop rapidly with distance so that beyond ~6 R_S there are probably very limited additional sources and losses. Thus, beyond these source regions, one can calculate the radial transport rate from conservation of mass and the radial density profile:

$$\text{Flux} = \text{Mdot} = M(R)\ V_r(R) \tag{8}$$

where V_r is the radial outflow speed, Mdot is the net plasma source, and $M(R)$ (in kilograms per meter) is the mass density integrated azimuthally and vertically, as shown in Figure 7.

[44] The net rate of radial transport can then be calculated as $V_r(R) = \text{Mdot}/M(R)$ as illustrated in Figure 10 for two values that span the range of Mdot for both Jupiter and Saturn. At Saturn the radial transport rate remains small (<10 km/s) but becomes significant (>40 km/s) beyond ~15 R_S for the highest plasma production rates. These values are fairly consistent with observations of *Wilson et al.* [2008] and simulations of *Liu et al.* [2010]. For Jupiter, when the plasma production is high, the radial transport rates can become a significant fraction of the local azimuthal flow speed (~200 km/s) beyond 40–50 R_J, and the plasma rapidly spirals out of the system [*Delamere and Bagenal*, 2010]. It should be noted that we are taking a single density profile across the factor of ~5 range in mass transport rate. Realistically, the density profile is likely to be modified with persistent enhancements or decreases in source rate at Io or Enceladus.

Table 5. Energy Flow Through the Magnetospheres of Jupiter and Saturn

	Jupiter	Saturn	J/S
Total kinetic energy (equation (9))	7.5×10^{18} J	8×10^{16} J	90
Power: kinetic energy	1.4–7.8 TW[a]	25–200 GW[a]	7–300
Total thermal energy (equation (10))	1×10^{18} J	1×10^{17} J	12
Power: plasma thermal energy	0.3–1.4 TW[a]	30–230 GW[a]	1–50
Total energetic ion energy (equation (11))	1.4×10^{19} J	1.6×10^{17} J	90
Power: energetic ion energy	2.7–15 TW[a]	45–400 GW[a]	7–300
Net heating of plasma disk	3–16 TW	75–630 GW	5–200
Power: solar wind[b]	130 TW	3 TW	40
Power: UV torus emission	1.2–2.5 TW	1.2 GW	1000–2000
Power: aurora	200–800 GW	10–30 GW	7–80
Power: magnetotail flows	1 TW	??	??
Power: satellite interaction	1 TW	0.3 GW	3000
Power: satellite aurora	6 GW	10 MW	600

[a]Assuming a range in time scales of 11–60 and 5–40 days for Jupiter and Saturn, respectively

[b]About 1% kinetic energy flux of solar wind onto area of πR_T^2, where R_T is the magnetopause distance at terminator (~120 R_J, ~38 R_S).

[45] This radial transport speed can be integrated to give typical transport time scales. The slower/faster transport rate results in longer/shorter time scales. Interestingly, a similar range of time scales (1–9 weeks) is found at both planets. Plasma diffusing outward spends most of the time in the plasma source regions (<7 R_J, < 9 R_S) where the transport rate is relatively slow.

3.5. Tailward Transport

[46] The plasma rotates around the planet and is slowly transported outward. At some point either the coupling to the planet breaks down completely (*Kivelson and Southwood* [2005] suggest via ballooning mode instability) or the field becomes so radially extended that an X point develops and a blob of plasma detaches and escapes down the magnetotail, as proposed by *Vasyliūnas* [1983]. Pursuing evidence for Vasyliūnas' argument that plasmoids are ejected down the tail, *Grodent et al.* [2004] found evidence of spots of auroral emission poleward of the main aurora connected to the nightside magnetosphere that flash with an approximately 10 min duration. Such events were rare, recurring only about once per 1–2 days. These flashes seemed to occur in the premidnight sector, and *Grodent et al.* [2004] estimated that they are coupled to a region of the magnetotail that was about 5–50 R_J across and located greater than 100 R_J down the tail. Studies of in situ measurements [*Russell et al.*, 2000; *Woch et al.*, 2002; *Ge et al.*, 2010; *Vogt et al.*, 2010] lead to conclusions that plasmoids on the order of ~25 R_J in scale are ejected every 4 h to 3 days, with a predominance for the postmidnight sector and distances of 70–120 R_J. Could such plasmoids account for most of the plasma loss down the magnetotail? *Bagenal* [2007] presented the following estimate: if one approximates a plasmoid to be a disk of 10 R_J thick plasma sheet that has a diameter of 25 R_J and a density of 0.01 cm^{-3}, then each plasmoid has a mass of about 2500 t; Ejecting one such plasmoid per day is equivalent to losing 0.03 t/s or 30 kg/s; Thus, even with generous numbers, the loss of plasma from the magnetosphere due to such plasmoid ejections cannot match (by a factor of ~20) the canonical plasma production rate of 500 kg/s; On the other hand, a steady flow of plasma of density 0.01 cm^{-3} in a conduit that is 2 R_J thick by 300 R_J wide moving at a speed of 200 km/s would provide a loss of 0.5 t/s. Such numbers suggest such a quasi-steady loss rate is feasible. The question of the mechanism remains unanswered. Three options are a diffusive "drizzle" across weak, highly stretched magnetotail fields, particularly on the dusk flank (as suggested by *Kivelson and Southwood* [2005]); a quasi-steady ejection of small plasmoids (below the scale detectable via auroral emissions); or a planetary wind along opened field lines (though this begs the questions of processes and time scales for opening, closing and refilling).

[47] At Saturn, to date only three plasmoid events have been reported from in situ data [*Jackman et al.*, 2007]. *McAndrews et al.* [2009] reported tailward flows on the postmidnight sector beyond 50 R_S. Further suggestion of possible plasmoid ejection has been inferred from bursts of ENAs that are correlated with Saturn Kilometric Radio emissions [*Mitchell et al.*, 2005; *Hill et al.*, 2008]. But it is not clear whether such plasmoids could remove the necessary 8–250 kg/s. Plasmoids of volume (10 R_S)^3 with density of 0.01 cm^{-3} of 18 amu ions would need to be ejected at a rate of 200/d to remove 100 kg/s. Thus, we have a similar issue at Saturn whereby much of the material has to be lost either through small-scale processes and/or out of the flanks of the magnetotail.

4. Energy: Distribution, Sources, and Flux

[48] With a simple model of the distribution of plasma mass, temperature and flows we can estimate the distribution, sources and flux of energy, summarized in Table 5. First, we discuss the energy budget of the main plasma source regions, the plasma tori of Io and Enceladus. Then we follow the plasma out into the magnetodisk and estimate the energy that must be added to the system to produce the observed plasma energies.

4.1. Torus Energy Budgets

[49] Figures 8 (bottom) and 9 (bottom) show the flow of energy through the Io and Enceladus plasma tori derived from equilibrium physical chemistry models. The main source of energy (~0.6–2.2 TW for Jupiter, ~30 GW for Saturn) comes from the gyromotion picked up by a newly ionized ion. While charge exchange does not contribute to the net plasma density, at both giant planets it is a larger source of energy than ionization. At Saturn most of this energy is then carried away by fast neutrals on subsequent charge exchange reactions. At both Jupiter and Saturn, little of the energy (~10%) is transported out into the plasma sheet, except when the source is particularly high, such as at the time of the Cassini outburst in fall 2000 (Figure 8) when nearly a quarter of the torus energy was transported into the plasma sheet. With the high plasma densities in the Io plasma torus the ions couple their pickup energy to electrons via Coulomb collisions, cooling the ions below the local pickup energies (270 and 540 eV for O^+ and S^+, respectively). But the electrons also excite the ions and this energy is quickly lost through the powerful UV emissions. At Saturn, the lower plasma density means that the ion-electron

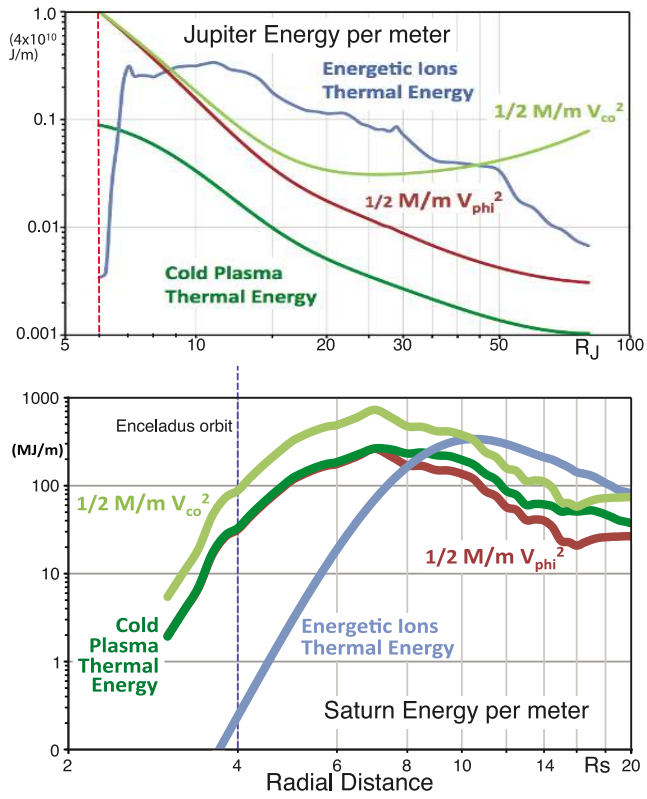

Figure 11. Radial profiles of energy density for (top) Jupiter and (bottom) Saturn.

coupling is weak and radiative cooling is insignificant for the Enceladus torus.

[50] Early models of the Io plasma torus showed that there was insufficient power provided from ion pickup alone to fuel the UV emissions [*Shemansky*, 1987]. A solution to this energy crisis was to add energy via a small population of hot electrons at energies of 40–100 eV [*Barbosa*, 1994; *Delamere and Bagenal*, 2003]. Under most torus conditions (at least, three of the 4 cases considered in Figure 8) hot electrons are needed to supply ~10–20% of the power. But to match the conditions in the later part of the Cassini flyby (spring 2001), over 60% of the power to the Io torus was supplied by the hot electrons, which then excited the ions and generated 1.5 TW of UV emission. Thus, in addition to local pick up energy, models of the Io torus need to add 0.2 to 0.9 TW via a source of hot electrons. While a relatively small fraction of the total electron population, the actual source of this population of hot electrons has yet to be determined but may be related to small-scale field-aligned currents concomitant with flux tube interchange. Moreover, *Steffl et al.* [2008] showed that variations in the hot electron population could explain the observed System III and IV modulations of torus emissions.

[51] At Saturn, the hot electrons provide an insubstantial fraction (~2%) of the power to the system but they are key for ionizing the neutral cloud [*Delamere et al.*, 2007; *Fleshman et al.*, 2010a, 2010b]. Modulation of this tiny population of hot electrons can strongly modulate the plasma density. *Delamere and Bagenal* [2008] argue that a longitudinal variation in hot electrons could be responsible for the longitudinal variations in the torus density around 4 R_S [*Gurnett et al.*, 2007].

4.2. Kinetic Energy

[52] The dominant flow in the magnetospheres of Jupiter and Saturn is rotational. Strict corotation at Jupiter is 12.6 R km/s and 9.8 R km/s at Saturn (where R is in planetary radii). Voyager data at Jupiter show a deviation from corotation, tending toward an azimuthal flow of about 200 km/s [*Belcher*, 1983, Figure 3.23]. Asymmetries in fluxes of energetic particles have been used to derive flows and show local time variations in these flows (see review by *Krupp et al.* [2004b]). We approximate the azimuthal flow in the Jovian plasma sheet with a simple function $V_{\mathrm{phi}} = V_{\mathrm{co}}\ (1.12 - R/50)$ up to ~200 km/s at ~28 R_J and a constant value of 200 km/s here on out (Table 1). At Saturn we approximate the azimuthal flow speeds derived by *Thomsen et al.* [2010, Figure 15] as $V_{\mathrm{phi}} = 0.6\ V_{\mathrm{co}}$.

[53] Combining the radial profiles of mass density, $M(R)$, and azimuthal flow (V_{phi}) we calculate the radial profile of kinetic energy (KE) (per meter of radial distance) of the plasma in the plasma disk

$$\mathrm{KE} = 1/2\ M(R)\ V_{\mathrm{phi}}^2 \tag{9}$$

which is shown for both Jupiter and Saturn in Figure 11.

[54] The kinetic energy of the thermal plasma drops with radial distance is a result of increasing subcorotation (in the case of Jupiter) and the drop in mass density with distance. Integrating equation (9) over the radial extent of the disk we get the net kinetic energy of ~7.5×10^{18} J at Jupiter, 8×10^{16} J at Saturn. Dividing this net kinetic energy of the disk by typical times scales for slow transport (60 days at Jupiter, 40 days at Saturn) and fast transport (11 days at Jupiter, perhaps as short as 5 days at Saturn), we obtain the power needed to keep the plasma disk rotating of 1.4–7.8 TW at Jupiter and 25–200 GW at Saturn. This energy comes ultimately from the planet's spin, coupled via field-aligned currents.

4.3. Thermal Energy

[55] Multiplying the local thermal energy density and volume of an annulus we obtain a radial profile of thermal energy (TE) of the plasma

$$\mathrm{TE}_{\mathrm{thermal}} = 3/2\ n_0 kT\ 2\pi^{3/2}\ H\ R \tag{10}$$

As shown in Figure 11, at Saturn, the thermal energy of the plasma tracks the kinetic energy out to about 7 R_S, consistent with the plasma being picked up at the local pickup energy with little outward transport of plasma and with local recombination and charge exchange losses balancing local sources. At Jupiter, the thermal energy remains well below the local pickup energy because much of the energy that is picked up on ionization and charge exchange is radiated away in the torus.

[56] We integrate this radial profile of thermal energy of the plasma to get the total thermal energy of the disk of 1×10^{18} J at Jupiter and 1×10^{17} J at Saturn. Again, we can use the radial transport time scales to obtain estimates of the power needed to heat the plasma this amount of

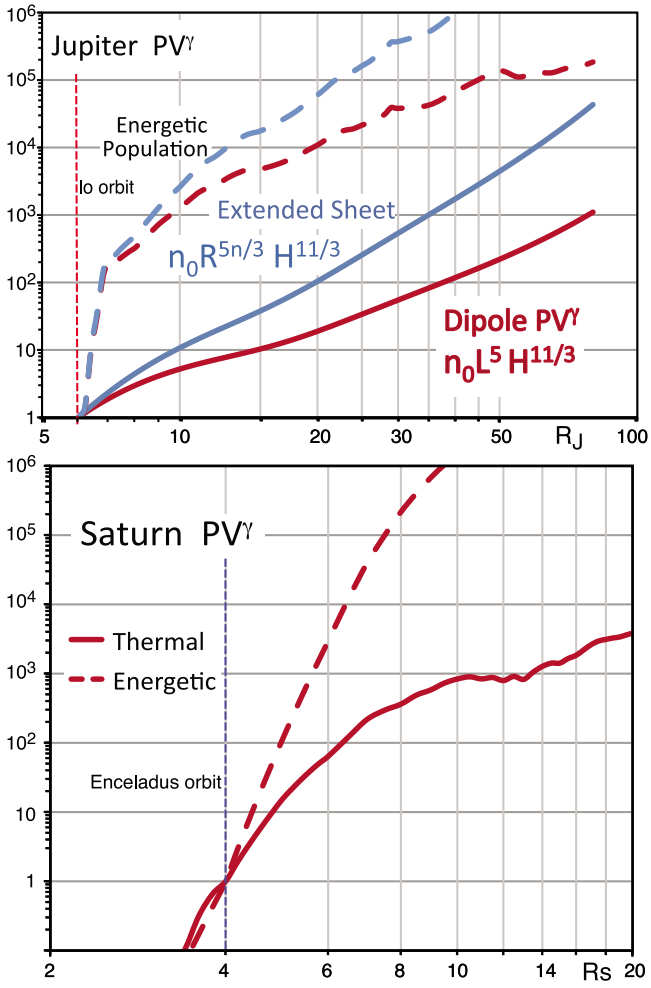

Figure 12. Radial profiles of quantities conserved for adiabatic motions for (top) Jupiter (normalized to value at 6 R_J) and (bottom) Saturn (normalized to value at 4 R_S). For the nondipole, extended field at Jupiter n = 3.85 [*Vogt et al.*, 2011].

0.3–1.4 TW at Jupiter and 30–230 GW at Saturn. This somewhat overestimates the actual energy needed to heat the plasma because it assumes the plasma retains none of its original energy as the plasma moves out, rather than cooling adiabatically on expansion. But since the expansion is dramatic and the observed thermal energy is large, the difference is insignificant.

[57] We can similarly estimate the energy density of the energetic particles as

$$\mathrm{TE_{hot}} = 3/2\ P_{\mathrm{hot}}\ 2\pi^{3/2}\ H\ R \tag{11}$$

Figure 11 shows that beyond ~9 R_J at Jupiter and ~9 R_S at Saturn the energetic particles dominate the energy density of the disk by about a factor of 10–20 at Jupiter and a factor 5–10 at Saturn. We integrate equation (11) over radial distance to values of 1.4 × 10^{19} J (Jupiter) and 1.6 × 10^{17} J (Saturn). The fact that we are ignoring that the hot population is probably less confined to the plasma sheet than the thermal population (i.e., H_{hot} is effectively larger than H_{thermal}) means that we are probably underestimating the thermal energy of this hot population. Nevertheless, we find total thermal energies of the suprathermal ions to be factors of ~2 that of the thermal populations at both Jupiter and Saturn.

[58] We use the radial transport time scales to obtain estimates of the power needed to heat the suprathermal ions to be 2.7–15 TW for Jupiter and 45–400 GW for Saturn.

[59] In summary, adding the power needed to heat both thermal and suprathermal populations in the plasma sheet one finds a net requirement of 3–16 TW at Jupiter and ~75–630 GW at Saturn. At Jupiter a further 0.2–1 TW must be supplied via hot electrons to the Io plasma torus.

4.4. Plasma Heating

[60] If plasma moves adiabatically within the magnetosphere then one would expect the quantity PV^{γ} to be conserved, where P is pressure, V is volume and γ is the ratio of specific heats, taken to be a value of 5/3 for a monotonic gas. For a dipole magnetic field and sheet geometry the volume of a magnetic flux shell varies as L^3H, where L is the dipole McIlwain parameter (e.g., derived in the appendix of *Richardson and Siscoe* [1983]). At Saturn the field is not so far from a dipole, making this approximation reasonable. At Jupiter, however, to obtain a more realistic, extended field geometry we use the radial variation in magnetic flux at the equator derived from Galileo data by *Vogt et al.* [2011], where the flux varies as $R^{-3.85}$ rather than R^{-3} of a dipole. For dipole geometry

$$PV^{\gamma} = PL^5H^{5/3} \tag{12}$$

and for the stretched plasma sheet we have

$$PV^{\gamma} = PR^{5n/3}H^{5/3} \tag{13}$$

where n = 3.85. Plotted in Figure 12 is PV^{γ} for both the thermal and hot particle populations, showing that this quantity is far from conserved at Jupiter, confirming that the plasma must be strongly heated. At Saturn, outside the source region (>8 R_S) the value of PV^{γ} remains fairly constant, suggesting adiabatic expansion, with heating of the thermal population not kicking in until ~15 R_S. The steep slopes for PV^{γ} of the energetic particle populations in Figure 12 illustrates their strong heating. *Mauk et al.* [1998] show significant depletion in energetic particle pressures from Voyager to Galileo and that the profiles of PV^{γ} of the energetic population became less steep, which they suggest may be due to greater charge exchange with a more extended neutral cloud.

[61] If one assumes that most of the mass from Jupiter's plasma sheet is lost via the ejection of material down the magnetotail then a simple calculation of 500 kg/s moving at ~200 km/s carries about ~1 TW of kinetic energy. As discussed in section 3.5, most of this energy must be carried in a background flow rather than in the episodic plasmoids producing detectable aurora.

[62] Table 5 compares the various kinds of energy and the power in and out of the two systems. Adding up the power that must be added to the plasma to (1) power the UV emissions; (2) heat the thermal plasma as it moves out from

the inner magnetosphere; (3) keep the disk rotating (albeit below full corotation); and (4) accelerate a substantial population of energetic particles, one obtains that the net power that must be added to be ~8–30 TW at Jupiter and ~0.1–0.9 TW at Saturn. These estimates are probably only one significant figure at best and the range gives an indication of the possible variability. Note that the total energy stored in the Jovian system is roughly 2 orders of magnitude greater than the Saturn system, primarily due to the much stronger Jovian magnetic field. On the other hand, the factor of 10 variability in the escape of volcanic material from Enceladus (compared with a factor of ~5 from Io) may produce occasions when Saturn's strongest volcanic outbursts match Jupiter's weakest epochs (Tables 2 and 5).

[63] While MHD models might be made to adequately account for processes 1 and 3, additional (perhaps ad hoc) processes will need to be added to account for 2 and 4. Some might argue that perhaps the process that heats the tens of keV particles (that remains unknown 30 years after the Pioneer era realization that such heating must occur) may occur on a different time scale than radial transport for the bulk of the plasma or that the energetic particles have a source in the outer magnetosphere and will gain energy as they move inward into stronger magnetic fields. Nevertheless, our estimates are probably within an order of magnitude of the power that needs to be added to the system to accelerate particles to observed energy densities.

[64] All of the above discussion assumes that the ultimate source of energy is the rotation of the planet, coupled to the magnetospheric plasma by the magnetic field. Another substantial source of energy is the kinetic energy of the solar wind. *Pu and Kivelson* [1983] estimate that about 1% of the solar wind kinetic energy is transferred to the magnetosphere. As we show in Table 5, just 1% of kinetic energy delivered to the magnetopause by the solar wind would swamp all of the above internal mechanisms. The issue is how to couple the energy from the solar wind, or even a boundary layer, to the internal plasma. Presumably, any KHI-mediated viscous interaction could transfer some of the solar wind kinetic energy to heating the outer layers of the magnetosphere (perhaps significantly at Saturn), but at Jupiter the iogenic heavy ions need to be heated deep inside the magnetosphere where solar wind influence is likely to be minimal.

5. Summary

[65] 1. The satellites Io and Enceladus fuel the giant magnetospheres of Jupiter and Saturn with neutral material at rates of hundreds to a few thousands of kilograms per second. The production at Io seems to be steadier (perhaps regulated by the magnetosphere-ionosphere interaction) and at the higher end of the range. The production by Enceladus tends to be rather less but more variable, perhaps related to the direct injection into the magnetosphere by the plumes. Furthermore, collisional processes in Saturn's dense neutral cloud spread the dissociated water products into a region that spans the inner half of the magnetosphere. Approximately one third to half of the iogenic neutrals becomes a net source of plasma, the remainder being lost from the system as fast neutrals. At Saturn the situation is more complicated with losses to ionization, to Saturn and its rings, and to escape. Currently, the relative importance of each process varies from model to model but the fact that an order of magnitude variation in plasma density has not yet been observed suggests that the rate of ionization does not keep up with the rate of production at Enceladus. Nevertheless, it is clear that a considerably smaller fraction of Saturn's neutral cloud becomes ionized and Saturn's plasma disk is dwarfed (in both scale and mass) by that of Jupiter.

[66] 2. Assuming the observed radial profiles of density are typical, we estimate the rate of radial transport of ionized material out of both systems to occur on time scales of ~1 to 9 weeks, with 20–60 days being more typical and the shorter time scale only perhaps occurring during periods of strong volcanic outbursts by Io or Enceladus.

[67] 3. The sources of energy at each planet comprise approximately similar contributions of rotational kinetic energy (of the heavy thermal plasma accelerated into rotation via coupling to the spinning planet), heating of the thermal plasma population, as well as acceleration of the substantial populations of energetic particles. Models aiming to capture the dynamics of these giant magnetospheres need to add a total heating power of 3–16 TW for Jupiter and 75–630 GW for Saturn to the plasmas in their magnetodisks.

[68] 4. While we have tried to quantify the total mass and energy flowing through the Jovian and Saturnian systems, four outstanding questions remain: (1) What physical processes provide the total power that is necessary to heat the plasma to observed energy densities? (2) Through what process is the plasma lost down the magnetotail? (3) What is the net source of mass, momentum and energy transferred from the solar wind to the magnetosphere? (4) What roles do local time and longitudinal asymmetries play in these processes?

[69] **Acknowledgments.** The authors are grateful for discussions with Margaret Kivelson, Tom Krimigis, Chris Paranicas, Joachim Saur, Tim Cassidy, Matt Burger, and Bobby Fleshman. F.B. thanks Steve Bartlett for assistance with making the figures. The authors acknowledge support from NASA's JDAP and CDAP.

References

Achilleos, N., P. Guio, C. S. Arridge, N. Sergis, R. J. Wilson, M. F. Thomsen, and A. J. Coates (2010), Influence of hot plasma pressure on the global structure of Saturn's magnetodisk, *Geophys. Res. Lett.*, *37*, L20201, doi:10.1029/2010GL045159.

Alexeev, I. I., and E. S. Belenkaya (2005), Modeling of the Jovian magnetosphere, *Ann. Geophys.*, *23*, 809–826, doi:10.5194/angeo-23-809-2005.

André, N., M. K. Dougherty, C. T. Russell, J. S. Leisner, and K. K. Khurana (2005), Dynamics of the Saturnian inner magnetosphere: First inferences from the Cassini magnetometers about small-scale plasma transport in the magnetosphere, *Geophys. Res. Lett.*, *32*, L14S06, doi:10.1029/2005GL022643.

Arridge, C. S., C. T. Russell, K. K. Khurana, N. Achilleos, N. André, A. M. Rymer, M. K. Dougherty, and A. J. Coates (2007), Mass of Saturn's magnetodisc: Cassini observations, *Geophys. Res. Lett.*, *34*, L09108, doi:10.1029/2006GL028921.

Arridge, C. S., C. T. Russell, K. K. Khurana, N. Achilleos, S. W. H. Cowley, M. K. Dougherty, D. J. Southwood, and E. J. Bunce (2008), Saturn's magnetodisc current sheet, *J. Geophys. Res.*, *113*, A04214, doi:10.1029/2007JA012540.

Bagenal, F. (1994), Empirical model of the Io plasma torus: Voyager measurements, *J. Geophys. Res.*, *99*, 11,043–11,062, doi:10.1029/93JA02908.

Bagenal, F. (2007), The magnetosphere of Jupiter: Coupling the equator to the poles, *J. Atmos. Sol. Terr. Phys.*, *69*, 387–402, doi:10.1016/j.jastp.2006.08.012.

Bagenal, F., and J. D. Sullivan (1981), Direct plasma measurements in the Io torus and inner magnetosphere of Jupiter, *J. Geophys. Res.*, *86*, 8447–8466, doi:10.1029/JA086iA10p08447.

Bagenal, F., T. Dowling, and B. McKinnon (Eds.) (2004), *Jupiter: Planet, Satellites, Magnetosphere*, Cambridge Univ. Press, Cambridge, U. K.

Bame, S. J., B. L. Barraclough, W. C. Feldman, G. R. Gisler, J. T. Gosling, D. J. McComas, J. L. Phillips, M. F. Thomsen, B. E. Goldstein, and M. Neugebauer (1992), Jupiter's magnetosphere: Plasma description from the Ulysses flyby, *Science*, *257*, 1539–1543, doi:10.1126/science.257.5076.1539.

Barbosa, D. D. (1994), Neutral cloud theory of the Jovian nebula: Anomalous ionization effect of superthermal electrons, *Astrophys. J.*, *430*, 376–386, doi:10.1086/174413.

Barbosa, D. D., D. A. Gurnett, W. S. Kurth, and F. L. Scarf (1979), Structure and properties of Jupiter's magnetoplasmadisc, *Geophys. Res. Lett.*, *6*(10), 785–788, doi:10.1029/GL006i010p00785.

Barnhart, B. L., W. S. Kurth, J. B. Groene, J. B. Faden, O. Santolik, and D. A. Gurnett (2009), Electron densities in Jupiter's outer magnetosphere determined from Voyager 1 and 2 plasma wave spectra, *J. Geophys. Res.*, *114*, A05218, doi:10.1029/2009JA014069.

Belcher, J. W. (1983), The low-energy plasma in the Jovian magnetosphere, in *Physics of the Jovian Magnetosphere*, edited by A. J. Dessler, pp. 68–105, Cambridge Univ. Press, Cambridge, U. K., doi:10.1017/CBO9780511564574.005.

Bolton, S. J., R. M. Thorne, D. A. Gurnett, W. S. Kurth, and D. J. Williams (1997), Enhanced whistler-mode emissions: Signatures of interchange motion in the Io torus, *Geophys. Res. Lett.*, *24*(17), 2123, doi:10.1029/97GL02020.

Borovsky, J. E., C. K. Goertz, and G. Joyce (1981), Magnetic pumping of particles in the outer Jovian magnetosphere, *J. Geophys. Res.*, *86*, 3481–3495, doi:10.1029/JA086iA05p03481.

Burch, J. L., J. Goldstein, T. W. Hill, D. T. Young, F. J. Crary, A. J. Coates, N. André, W. S. Kurth, and E. C. Sittler (2005), Properties of local plasma injections in Saturn's magnetosphere, *Geophys. Res. Lett.*, *32*, L14S02, doi:10.1029/2005GL022611.

Carbary, J. F., A. J. Dessler, and T. W. Hill (1976), Planetary spin period acceleration of particles in the Jovian magnetosphere, *J. Geophys. Res.*, *81*, 5189–5195, doi:10.1029/JA081i028p05189.

Cassidy, T. A., and R. E. Johnson (2010), Collisional spreading of Enceladus' neutral cloud, *Icarus*, *209*, 696–703, doi:10.1016/j.icarus.2010.04.010.

Caudal, G. (1986), A self-consistent model of Jupiter's magnetodisc including the effects of centrifugal force and pressure, *J. Geophys. Res.*, *91*, 4201–4221, doi:10.1029/JA091iA04p04201.

Chen, Y., and T. W. Hill (2008), Statistical analysis of injection/dispersion events in Saturn's inner magnetosphere, *J. Geophys. Res.*, *113*, A07215, doi:10.1029/2008JA013166.

Chen, Y., T. W. Hill, A. M. Rymer, and R. J. Wilson (2010), Rate of radial transport of plasma in Saturn's inner magnetosphere, *J. Geophys. Res.*, *115*, A10211, doi:10.1029/2010JA015412.

Chou, M., and C. Z. Cheng (2010), Modeling of Saturn's magnetosphere during Voyager 1 and Voyager 2 encounters, *J. Geophys. Res.*, *115*, A08202, doi:10.1029/2009JA015124.

Cohen, C. M. S., E. C. Stone, and R. Selesnick (2001), Energetic ion observations in the middle Jovian magnetosphere, *J. Geophys. Res.*, *106*, 29,871–29,881, doi:10.1029/2001JA000008.

Delamere, P. A., and F. Bagenal (2003), Modeling variability of plasma conditions in the Io torus, *J. Geophys. Res.*, *108*(A7), 1276, doi:10.1029/2002JA009706.

Delamere, P. A., and F. Bagenal (2008), Longitudinal density variations at Saturn caused by hot electrons, *Geophys. Res. Lett.*, *35*, L03107, doi:10.1029/2007GL031095.

Delamere, P. A., and F. Bagenal (2010), Modeling the Enceladus plume-plasma interaction: Solar wind-driven flows in Jupiter's magnetosphere, *J. Geophys. Res.*, *115*, A10201, doi:10.1029/2010JA015347.

Delamere, P. A., A. Steffl, and F. Bagenal (2004), Modeling temporal variability of plasma conditions in the Io torus during the Cassini era, *J. Geophys. Res.*, *109*, A10216, doi:10.1029/2003JA010354.

Delamere, P. A., F. Bagenal, V. Dols, and L. Ray (2007), Saturn's neutral torus vs. Jupiter's plasma torus, *Geophys. Res. Lett.*, *34*, L09105, doi:10.1029/2007GL029437.

Dessler, A. J. (Ed.) (1983), *Physics of the Jovian Magnetosphere*, Cambridge Univ. Press, Cambridge, U. K., doi:10.1017/CBO9780511564574.

Dougherty, M., L. Esposito, and S. Krimigis (Eds.) (2009), *Saturn From Cassini-Huygens*, Springer, New York, doi:10.1007/978-1-4020-9217-6.

Ebert, R. W., D. J. McComas, F. Bagenal, and H. A. Elliott (2010), Location, structure, and motion of Jupiter's dusk magnetospheric boundary from ~625 to 2550 R_J, *J. Geophys. Res.*, *115*, A12223, doi:10.1029/2010JA015938.

Fleshman, B. L., P. A. Delamere, and F. Bagenal (2010a), Modeling the Enceladus plume-plasma interaction, *Geophys. Res. Lett.*, *37*, L03202, doi:10.1029/2009GL041613.

Fleshman, B. L., P. A. Delamere, and F. Bagenal (2010b), A sensitivity study of the Enceladus torus, *J. Geophys. Res.*, *115*, E04007, doi:10.1029/2009JE003372.

Fleshman, B. L., P. A. Delamere, and F. Bagenal (2010c), The source of Saturn's extended neutral cloud, Abstract SM11C-1768 presented at 2010 Fall Meeting, AGU, San Francisco, Calif., 13–17 Dec.

Frank, L. A., and W. R. Paterson (2000), Observations of plasmas in the Io plasma torus with the Galileo spacecraft, *J. Geophys. Res.*, *105*, 16,017–16,034, doi:10.1029/1999JA000250.

Frank, L. A., W. R. Paterson, and K. K. Khurana (2002), Observations of thermal plasmas in Jupiter's magnetotail, *J. Geophys. Res.*, *107*(A1), 1003, doi:10.1029/2001JA000077.

Fujimoto, M., and A. Nishida (1990), Monte Carlo simulation of energization of Jovian trapped electrons by recirculation, *J. Geophys. Res.*, *95*, 3841–3853, doi:10.1029/JA095iA04p03841.

Fukazawa, K., T. Ogino, and R. J. Walker (2005), Dynamics of the Jovian magnetosphere for northward interplanetary magnetic field (IMF), *Geophys. Res. Lett.*, *32*, L03202, doi:10.1029/2004GL021392.

Fukazawa, K., T. Ogino, and R. J. Walker (2006), Configuration and dynamics of the Jovian magnetosphere, *J. Geophys. Res.*, *111*, A10207, doi:10.1029/2006JA011874.

Fukazawa, K., T. Ogino, and R. J. Walker (2010), A simulation study of dynamics in the distant Jovian magnetotail, *J. Geophys. Res.*, *115*, A09219, doi:10.1029/2009JA015228.

Galvin, A. B., C. M. S. Cohen, F. M. Ipavich, R. von Steiger, J. Woch, and U. Mall (1993), Boundary layer ion composition at Jupiter during the inbound pass of the Ulysses flyby, *Planet. Space Sci.*, *41*, 869–876, doi:10.1016/0032-0633(93)90094-I.

Ge, Y. S., C. T. Russell, and K. K. Khurana (2010), Reconnection sites in Jupiter's magnetotail and relation to Jovian auroras, *Planet. Space Sci.*, *58*, 1455–1469, doi:10.1016/j.pss.2010.06.013.

Glocer, A., G. Tóth, T. Gombosi, and D. Welling (2009), Modeling ionospheric outflows and their impact on the magnetosphere, initial results, *J. Geophys. Res.*, *114*, A05216, doi:10.1029/2009JA014053.

Goertz, C. K. (1976), The current sheet in Jupiter's magnetosphere, *J. Geophys. Res.*, *81*, 3368–3372, doi:10.1029/JA081i019p03368.

Goertz, C. K. (1978), Energization of charged particles in Jupiter's outer magnetosphere, *J. Geophys. Res.*, *83*, 3145–3150, doi:10.1029/JA083iA07p03145.

Goertz, C. K. (1983), Detached plasma in Saturn's front side magnetosphere, *Geophys. Res. Lett.*, *10*, 455, doi:10.1029/GL010i006p00455.

Gombosi, T. I., and K. C. Hansen (2005), Saturn's variable magnetosphere, *Science*, *307*, 1224–1226, doi:10.1126/science.1108226.

Grodent, D., J.-C. Gérard, J. T. Clarke, G. R. Gladstone, and J. H. Waite (2004), A possible auroral signature of a magnetotail reconnection process on Jupiter, *J. Geophys. Res.*, *109*, A05201, doi:10.1029/2003JA010341.

Gurnett, D. A., A. M. Persoon, W. S. Kurth, J. B. Groene, T. F. Averkamp, M. K. Dougherty, and D. J. Southwood (2007), The variable rotation period of the inner region of Saturn's plasma disk, *Science*, *316*, 442, doi:10.1126/science.1138562.

Haggerty, D. K., M. E. Hill, R. L. McNutt Jr., and C. Paranicas (2009), Composition of energetic particles in the Jovian magnetotail, *J. Geophys. Res.*, *114*, A02208, doi:10.1029/2008JA013659.

Hamilton, D. C., G. Gloeckler, S. M. Krimigis, and L. J. Lanzerotti (1981), Composition of nonthermal ions in the Jovian magnetosphere, *J. Geophys. Res.*, *86*, 8301–8318, doi:10.1029/JA086iA10p08301.

Hansen, K. C., A. J. Ridley, G. B. Hospodarsky, N. Achilleos, M. K. Dougherty, T. I. Gombosi, and G. Tóth (2005), Global MHD simulations of Saturn's magnetosphere at the time of Cassini approach, *Geophys. Res. Lett.*, *32*, L20S06, doi:10.1029/2005GL022835.

Hansen, C. J., L. Esposito, A. I. F. Stewart, J. Colwell, A. Hendrix, W. Pryor, D. Shemansky, and R. West (2006), Enceladus' water vapor plume, *Science*, *311*, 1422–1425, doi:10.1126/science.1121254.

Hansen, C. J., L. W. Esposito, A. I. F. Stewart, B. Meinke, B. Wallis, J. E. Colwell, A. R. Hendrix, K. Larsen, W. Pryor, and F. Tian (2008), Water vapour jets inside the plume of gas leaving Enceladus, *Nature*, *456*, 477–479, doi:10.1038/nature07542.

Hansen, C. J., D. E. Shemansky, L. W. Esposito, A. I. F. Stewart, and A. R. Hendrix (2010), The composition and structure of Enceladus' plume from a Cassini UVIS observation of a solar occultation, Abstract P23C-09 presented at 2010 Fall Meeting, AGU, San Francisco, Calif., 13–17 Dec.

Hill, T. W., and F. C. Michel (1976), Heavy ions from the Galilean satellites and the centrifugal distortion of the Jovian magnetosphere, *J. Geophys. Res.*, *81*, 4561, doi:10.1029/JA081i025p04561.

Hill, M. E., D. K. Haggerty, R. L. McNutt, and C. P. Paranicas (2009), Energetic particle evidence for magnetic filaments in Jupiter's magnetotail, *J. Geophys. Res.*, *114*, A11201, doi:10.1029/2009JA014374.

Hill, T. W., A. J. Dessler, and L. J. Maher (1981), Corotating magnetospheric convection, *J. Geophys. Res.*, *86*, 9020–9028, doi:10.1029/JA086iA11p09020.

Hill, T. W., A. J. Dessler, and C. K. Goertz (1983), Magnetospheric models, in *Physics of the Jovian Magnetosphere*, edited by A. J. Dessler, pp. 353–394, Cambridge Univ. Press, New York, doi:10.1017/CBO9780511564574.012.

Hill, T. W., A. M. Rymer, J. L. Burch, F. J. Crary, D. T. Young, M. F. Thomsen, D. Delapp, N. André, A. J. Coates, and G. R. Lewis (2005), Evidence for rotationally driven plasma transport in Saturn's magnetosphere, *Geophys. Res. Lett.*, *32*, L14S10, doi:10.1029/2005GL022620.

Hill, T. W., et al. (2008), Plasmoids in Saturn's magnetotail, *J. Geophys. Res.*, *113*, A01214, doi:10.1029/2007JA012626.

Huddleston, D. E., C. T. Russell, M. G. Kivelson, K. K. Khurana, and L. Bennett (1998), Location and shape of the Jovian magnetopause and bow shock, *J. Geophys. Res.*, *103*, 20,075–20,082, doi:10.1029/98JE00394.

Jackman, C. M., C. T. Russell, D. J. Southwood, C. S. Arridge, N. Achilleos, and M. K. Dougherty (2007), Strong rapid dipolarizations in Saturn's magnetotail: In situ evidence of reconnection, *Geophys. Res. Lett.*, *34*, L11204, doi:10.1029/2007GL029764.

Joy, S. P., M. G. Kivelson, R. J. Walker, K. K. Khurana, C. T. Russell, and T. Ogino (2002), Probabilistic models of the Jovian magnetopause and bow shock locations, *J. Geophys. Res.*, *107*(A10), 1309, doi:10.1029/2001JA009146.

Jurac, S., and J. D. Richardson (2005), A self-consistent model of plasma and neutrals at Saturn: Neutral cloud morphology, *J. Geophys. Res.*, *110*, A09220, doi:10.1029/2004JA010635.

Kanani, S. J., et al. (2010), A new form of Saturn's magnetopause using a dynamic pressure balance model, based on in situ, multi-instrument Cassini measurements, *J. Geophys. Res.*, *115*, A06207, doi:10.1029/2009JA014262.

Kellett, S., C. S. Arridge, E. J. Bunce, A. J. Coates, S. W. H. Cowley, M. K. Dougherty, A. M. Persoon, N. Sergis, and R. J. Wilson (2010), Nature of the ring current in Saturn's dayside magnetosphere, *J. Geophys. Res.*, *115*, A08201, doi:10.1029/2009JA015146.

Kivelson, M. G., and D. J. Southwood (2005), Dynamical consequences of two modes of centrifugal instability in Jupiter's outer magnetosphere, *J. Geophys. Res.*, *110*, A12209, doi:10.1029/2005JA011176.

Kivelson, M. G., K. K. Khurana, C. T. Russell, and R. J. Walker (1997), Intermittent short-duration magnetic field anomalies in the Io torus: Evidence for plasma interchange?, *Geophys. Res. Lett.*, *24*(17), 2127–2130, doi:10.1029/97GL02202.

Krimigis, S. M., and E. C. Roelof (1983), Low-energy particle population, in *Physics of the Jovian Magnetosphere*, edited by A. J. Dessler, pp. 106–156, Cambridge Univ. Press, New York, doi:10.1017/CBO9780511564574.006.

Krimigis, S. M., J. F. Carbary, E. P. Keath, C. O. Bostrom, W. I. Axford, G. Gloeckler, L. J. Lanzerotti, and T. P. Armstrong (1981), Characteristics of hot plasma in the Jovian magnetosphere: Results from the Voyager spacecraft, *J. Geophys. Res.*, *86*, 8227–8257, doi:10.1029/JA086iA10p08227.

Krimigis, S. M., et al. (2005), Dynamics of Saturn's magnetosphere from MIMI during Cassini's orbital insertion, *Science*, *307*, 1270, doi:10.1126/science.1105978.

Krüger, H., P. Geissler, M. Horanyi, A. L. Graps, S. Kempf, R. Srama, G. Moragas-Klostermeyer, R. Moissl, T. V. Johnson, and E. Grun (2003), Jovian dust streams: A monitor of Io's volcanic plume activity, *Geophys. Res. Lett.*, *30*(21), 2101, doi:10.1029/2003GL017827.

Krupp, N., et al. (2004a), Energetic particle observations in the vicinity of Jupiter: Cassini MIMI/LEMMS results, *J. Geophys. Res.*, *109*, A09S10, doi:10.1029/2003JA010111.

Krupp, N., et al. (2004b), Dynamics of the Jovian magnetosphere, in *Jupiter: The Planet, Satellites, and Magnetosphere*, edited by F. Bagenal, T. E. Dowling, and W. B. McKinnon, pp. 617–638, Cambridge Univ. Press, Cambridge, U. K.

Lichtenberg, G., and N. Thomas (2001), Detection of S (IV) 10.51 μm emission from the Io plasma torus, *J. Geophys. Res.*, *106*, 29,899–29,910, doi:10.1029/2001JA900020.

Liu, X., T. W. Hill, R. A. Wolf, S. Sazykin, R. W. Spiro, and H. Wu (2010), Numerical simulation of plasma transport in Saturn's inner magnetosphere using the Rice Convection Model, *J. Geophys. Res.*, *115*, A12254, doi:10.1029/2010JA015859.

Masters, A., N. Achilleos, C. Bertucci, M. K. Dougherty, S. J. Kanani, C. S. Arridge, H. J. McAndrews, and A. J. Coates (2009), Surface waves on Saturn's dawn flank magnetopause driven by the Kelvin-Helmholtz instability, *Planet. Space Sci.*, *57*, 1769–1778, doi:10.1016/j.pss.2009.02.010.

Mauk, B. H., and S. M. Krimigis (1987), Radial force balance within Jupiter's dayside magnetosphere, *J. Geophys. Res.*, *92*, 9931–9941, doi:10.1029/JA092iA09p09931.

Mauk, B. H., et al. (1998), Galileo-measured depletion of near-Io hot ring current plasmas since the Voyager epoch, *J. Geophys. Res.*, *103*, 4715–4722, doi:10.1029/97JA02343.

Mauk, B. H., D. G. Mitchell, S. M. Krimigis, E. C. Roelof, and C. P. Paranicas (2003), Energetic neutral atoms from a trans-Europa gas torus at Jupiter, *Nature*, *421*, 920–922, doi:10.1038/nature01431.

Mauk, B. H., D. G. Mitchell, R. W. McEntire, C. P. Paranicas, E. C. Roelof, D. J. Williams, S. M. Krimigis, and A. Lagg (2004), Energetic ion characteristics and neutral gas interactions in Jupiter's magnetosphere, *J. Geophys. Res.*, *109*, A09S12, doi:10.1029/2003JA010270.

Mauk, B. H., et al. (2005), Energetic particle injections in Saturn's magnetosphere, *Geophys. Res. Lett.*, *32*, L14S05, doi:10.1029/2005GL022485.

McAndrews, H. J., et al. (2009), Plasma in Saturn's nightside magnetosphere and the implications for global circulation, *Planet. Space Sci.*, *57*, 1714–1722, doi:10.1016/j.pss.2009.03.003.

McComas, D. J., and F. Bagenal (2007), Jupiter: A fundamentally different magnetospheric interaction with the solar wind, *Geophys. Res. Lett.*, *34*, L20106, doi:10.1029/2007GL031078.

McNutt, R. L. (1984), Force balance in outer planet magnetospheres, in *Physics of Space Plasmas, Proceedings of the 1982–4 MIT Symposia, SPI Conf. Proc. Reprint Ser*., vol. 5, edited by J. Belcher et al., pp. 179–210, Scientific, Jodhpur, India.

McNutt, R. L., J. W. Belcher, and H. S. Bridge (1981), Positive ion observations in the middle magnetosphere of Jupiter, *J. Geophys. Res.*, *86*, 8319–8342, doi:10.1029/JA086iA10p08319.

Melin, H., D. E. Shemansky, and X. Liu (2009), The distribution of atomic hydrogen and oxygen in the magnetosphere of Saturn, *Planet. Space Sci.*, *57*, 1743–1753, doi:10.1016/j.pss.2009.04.014.

Mitchell, D. G., et al. (2005), Energetic ion acceleration in Saturn's magnetotail: Substorms at Saturn?, *Geophys. Res. Lett.*, *32*, L20S01, doi:10.1029/2005GL022647.

Morooka, M. W., et al. (2009), The electron density of Saturn's magnetosphere, *Ann. Geophys.*, *27*, 2971–2991, doi:10.5194/angeo-27-2971-2009.

Nagy, A. F., A. R. Barakat, and R. W. Schunk (1986), Is Jupiter's ionosphere a significant plasma source for its magnetosphere?, *J. Geophys. Res.*, *91*, 351–354, doi:10.1029/JA091iA01p00351.

Nishida, A. (1976), Outward diffusion of energetic particles from the Jovian radiation belt, *J. Geophys. Res.*, *81*, 1771–1773, doi:10.1029/JA081i010p01771.

Paranicas, C. P., B. H. Mauk, and S. M. Krimigis (1991), Pressure anisotropy and radial stress balance in the Jovian neutral sheet, *J. Geophys. Res.*, *96*, 21,135–21,140, doi:10.1029/91JA01647.

Persoon, A. M., et al. (2009), A diffusive equilibrium model for the plasma density in Saturn's magnetosphere, *J. Geophys. Res.*, *114*, A04211, doi:10.1029/2008JA013912.

Phillips, J. L., S. J. Bame, B. L. Barraclough, D. J. McComas, R. J. Forsyth, P. Canu, and P. J. Kellogg (1993), Ulysses plasma electron observations in the Jovian magnetosphere, *Planet. Space Sci.*, *41*, 877–892, doi:10.1016/0032-0633(93)90095-J.

Pontius, D., and T. W. Hill (2009), Inertial corotation lag and mass loading in Saturn's magnetosphere, *Geophys. Res. Lett.*, *36*, L23103, doi:10.1029/2009GL041030.

Pu, Z., and M. G. Kivelson (1983), Kelvin-Helmholtz instability at the magnetopause: Energy flux into the magnetosphere, *J. Geophys. Res.*, *88*, 853–861, doi:10.1029/JA088iA02p00853.

Richardson, J. D. (1986), Thermal ions at Saturn: Plasma parameters and implications, *J. Geophys. Res.*, *91*, 1381–1389, doi:10.1029/JA091iA02p01381.

Richardson, J. D., and G. L. Siscoe (1983), The problem of cooling the cold Io torus, *J. Geophys. Res.*, *88*, 2001–2009, doi:10.1029/JA088iA03p02001.

Richardson, J. D., and E. C. Sittler (1990), A plasma density model for Saturn based on Voyager observations, *J. Geophys. Res.*, *95*, 12,019–12,031, doi:10.1029/JA095iA08p12019.

Russell, C. T., M. G. Kivelson, K. K. Khurana, and D. E. Huddleston (2000), Circulation and dynamics in the Jovian magnetosphere, *Adv. Space Res.*, *26*, 1671–1676, doi:10.1016/S0273-1177(00)00115-0.

Saur, J. (2004), Turbulent heating of Jupiter's middle magnetosphere, *Astrophys. J.*, *602*, L137–L140, doi:10.1086/382588.

Saur, J., N. Schilling, F. M. Neubauer, D. F. Strobel, S. Simon, M. K. Dougherty, C. T. Russell, and R. T. Pappalardo (2008), Evidence for temporal variability of Enceladus' gas jets: Modeling of Cassini observation, *Geophys. Res. Lett.*, *35*, L20105, doi:10.1029/2008GL035811.

Schardt, A. W., and C. K. Goertz (1983), High-energy particles, in *of the Jovian Magnetosphere*, edited by A. J. Dessler, pp. 156–196, Cambridge Univ. Press, doi:10.1017/CBO9780511564574.007.

Schippers, P., et al. (2008), Multi-instrument analysis of electron populations in Saturn's magnetosphere, *J. Geophys. Res.*, *113*, A07208, doi:10.1029/2008JA013098.

Schreier, R., A. Eviatar, and V. M. Vasyliūnas (1998), A two-dimensional model of plasma transport and chemistry in the Jovian magnetosphere, *J. Geophys. Res.*, *103*, 19,901–19,913, doi:10.1029/98JE00697.

Scudder, J. D., E. C. Sittler, and H. S. Bridge (1981), A survey of the plasma electron environment of Jupiter: A view from Voyager, *J. Geophys. Res.*, *86*, 8157–8179, doi:10.1029/JA086iA10p08157.

Selesnick, R. S., C. M. S. Cohen, and K. K. Khurana (2001), Energetic ion dynamics in Jupiter's plasma sheet, *J. Geophys. Res.*, *106*, 18,895–18,905, doi:10.1029/2000JA000242.

Sentman, D. D., J. A. van Allen, and C. K. Goertz (1975), Recirculation of energetic particles in Jupiter's magnetosphere, *Geophys. Res. Lett.*, *2*, 465–468, doi:10.1029/GL002i010p00465.

Sergis, N., S. M. Krimigis, D. G. Mitchell, D. C. Hamilton, N. Krupp, B. H. Mauk, E. C. Roelof, and M. K. Dougherty (2009), Energetic particle pressure in Saturn's magnetosphere measured with the Magnetospheric Imaging Instrument on Cassini, *J. Geophys. Res.*, *114*, A02214, doi:10.1029/2008JA013774.

Sergis, N., et al. (2010), Particle pressure, inertial force, and ring current density profiles in the magnetosphere of Saturn, based on Cassini measurements, *Geophys. Res. Lett.*, *37*, L02102, doi:10.1029/2009GL041920.

Shemansky, D. E. (1987), Ratio of oxygen to sulfur in the Io plasma torus, *J. Geophys. Res.*, *92*, 6141–6146, doi:10.1029/JA092iA06p06141.

Shemansky, D. E. (1988), Energy branching in the Io plasma torus: The failure of neutral cloud theory, *J. Geophys. Res.*, *93*, 1773–1784, doi:10.1029/JA093iA03p01773.

Shemansky, D. E., P. Matheson, D. T. Hall, H.-Y. Hu, and T. M. Tripp (1993), Detection of the hydroxyl radical in the Saturn magnetosphere, *Nature*, *363*, 329–331, doi:10.1038/363329a0.

Shemansky, D. E., X. Liu, and H. Melin (2009), The Saturn hydrogen plume, *Planet. Space Sci.*, *57*, 1659–1670, doi:10.1016/j.pss.2009.05.002.

Sittler, E. C., K. W. Ogilvie, and J. D. Scudder (1983), Survey of low-energy plasma electrons in Saturn's magnetosphere: Voyagers 1 and 2, *J. Geophys. Res.*, *88*, 8847–8870, doi:10.1029/JA088iA11p08847.

Sittler, E. C., et al. (2008), Ion and neutral sources and sinks within Saturn's inner magnetosphere: Cassini results, *Planet. Space Sci.*, *56*, 3–18, doi:10.1016/j.pss.2007.06.006.

Slavin, J. A., E. J. Smith, J. R. Spreiter, and S. S. Stahara (1985), Solar wind flow about the outer planets: Gas dynamic modeling of the Jupiter and Saturn bow shocks, *J. Geophys. Res.*, *90*, 6275–6286, doi:10.1029/JA090iA07p06275.

Smith, H. T., R. E. Johnson, M. E. Perry, D. G. Mitchell, R. L. McNutt, and D. T. Young (2010), Enceladus plume variability and the neutral gas densities in Saturn's magnetosphere, *J. Geophys. Res.*, *115*, A10252, doi:10.1029/2009JA015184.

Smyth, W. H., and M. L. Marconi (2005), Nature of the iogenic plasma source in Jupiter's magnetosphere II. Near-Io distribution, *Icarus*, *176*, 138–154, doi:10.1016/j.icarus.2005.01.010.

Steffl, A. J., F. Bagenal, and A. I. F. Stewart (2004), Cassini UVIS Observations of the Io Plasma Torus: I. Initial results, *Icarus*, *172*, 78–90, doi:10.1016/j.icarus.2003.12.027.

Steffl, A. J., P. A. Delamere, and F. Bagenal (2006), Cassini UVIS observations of the Io plasma torus. III. Modeling temporal and azimuthal variability, *Icarus*, *180*, 124–140, doi:10.1016/j.icarus.2005.07.013.

Steffl, A. J., P. A. Delamere, and F. Bagenal (2008), Cassini UVIS observations of the Io plasma torus. IV. Observations of temporal and azimuthal variability, *Icarus*, *194*, 153–165, doi:10.1016/j.icarus.2007.09.019.

Thomas, N., F. Bagenal, T. W. Hill, and J. K. Wilson (2004), The Io neutral clouds and plasma torus, in *Jupiter: The Planet, Satellites, and Magnetosphere*, edited by F. Bagenal, T. E. Dowling, and W. B. McKinnon, pp. 561–591, Cambridge Univ. Press, New York.

Thomsen, M. F., D. B. Reisenfeld, D. M. Delapp, R. L. Tokar, D. T. Young, F. J. Crary, E. C. Sittler, M. A. McGraw, and J. D. Williams (2010), Survey of ion plasma parameters in Saturn's magnetosphere, *J. Geophys. Res.*, *115*, A10220, doi:10.1029/2010JA015267.

Thorne, R. M., T. P. Armstrong, S. Stone, D. J. Williams, R. W. McEntire, S. J. Bolton, D. A. Gurnett, and M. G. Kivelson (1997), Galileo evidence for rapid interchange transport in the Io torus, *Geophys. Res. Lett.*, *24*, 2131–2134, doi:10.1029/97GL01788.

Tokar, R. L., R. E. Johnson, M. F. Thomsen, R. J. Wilson, D. T. Young, F. J. Crary, A. J. Coates, G. H. Jones, and C. S. Paty (2009), Cassini detection of Enceladus' cold water-group plume ionosphere, *Geophys. Res. Lett.*, *36*, L13203, doi:10.1029/2009GL038923.

Vasyliūnas, V. M. (1983), Plasma distribution and flow, in *Physics of the Jovian Magnetosphere*, edited by A. J. Dessler, pp. 395–453, Cambridge Univ. Press, New York, doi:10.1017/CBO9780511564574.013.

Vasyliūnas, V. M. (2008), Comparing Jupiter and Saturn: Dimensionless input rates from plasma sources within the magnetosphere, *Ann. Geophys.*, *26*, 1341–1343, doi:10.5194/angeo-26-1341-2008.

Vogt, M. F., M. G. Kivelson, K. K. Khurana, S. P. Joy, and R. J. Walker (2010), Reconnection and flows in the Jovian magnetotail as inferred from magnetometer observations, *J. Geophys. Res.*, *115*, A06219, doi:10.1029/2009JA015098.

Vogt, M. F., M. G. Kivelson, K. K. Khurana, R. J. Walker, B. Bonfond, D. Grodent, and A. Radioti (2011), Improved mapping of Jupiter's auroral features to magnetospheric sources, *J. Geophys. Res.*, *116*, A03220, doi:10.1029/2010JA016148.

Wilson, R. J., R. L. Tokar, M. G. Henderson, T. W. Hill, M. F. Thomsen, and D. H. Pontius (2008), Cassini plasma spectrometer thermal ion measurements in Saturn's inner magnetosphere, *J. Geophys. Res.*, *113*, A12218, doi:10.1029/2008JA013486.

Winglee, R. M., D. Snowden, and A. Kidder (2009), Modification of Titan's ion tail and the Kronian magnetosphere: Coupled magnetospheric simulations, *J. Geophys. Res.*, *114*, A05215, doi:10.1029/2008JA013343.

Woch, J., N. Krupp, and A. Lagg (2002), Particle bursts in the Jovian magnetosphere: Evidence for a near-Jupiter neutral line, *Geophys. Res. Lett.*, *29*(7), 1138, doi:10.1029/2001GL014080.

Zieger, B., K. C. Hansen, T. I. Gombosi, and D. L. De Zeeuw (2010), Periodic plasma escape from the mass-loaded Kronian magnetosphere, *J. Geophys. Res.*, *115*, A08208, doi:10.1029/2009JA014951.

F. Bagenal and P. A. Delamere, Laboratory for Atmospheric and Space Physics, University of Colorado at Boulder, Duane Physics UCB 392, Boulder, CO 80309-0392, USA. (bagenal@colorado.edu)